



---

**Biocompatible and Biomimetic Self-Assembly of Functional Nanostructures**

**Jeffrey Brinker**  
**UNIVERSITY OF NEW MEXICO**

---

**03/10/2017**  
**Final Report**

DISTRIBUTION A: Distribution approved for public release.

Air Force Research Laboratory  
AF Office Of Scientific Research (AFOSR)/ RTB2  
Arlington, Virginia 22203  
Air Force Materiel Command

<b>REPORT DOCUMENTATION PAGE</b>		<i>Form Approved</i> OMB No. 0704-0188	
<p>The public reporting burden for this collection of information is estimated to average 1 hour per response, including the time for reviewing instructions, searching existing data sources, gathering and maintaining the data needed, and completing and reviewing the collection of information. Send comments regarding this burden estimate or any other aspect of this collection of information, including suggestions for reducing the burden, to Department of Defense, Executive Services, Directorate (0704-0188). Respondents should be aware that notwithstanding any other provision of law, no person shall be subject to any penalty for failing to comply with a collection of information if it does not display a currently valid OMB control number.</p> <p><b>PLEASE DO NOT RETURN YOUR FORM TO THE ABOVE ORGANIZATION.</b></p>			
<b>1. REPORT DATE (DD-MM-YYYY)</b> 15-03-2017		<b>2. REPORT TYPE</b> Final Performance	
<b>3. DATES COVERED (From - To)</b> 01 Feb 2014 to 31 Jan 2017			
<b>4. TITLE AND SUBTITLE</b> Biocompatible and Biomimetic Self-Assembly of Functional Nanostructures		<b>5a. CONTRACT NUMBER</b>	
		<b>5b. GRANT NUMBER</b> FA9550-14-1-0066	
		<b>5c. PROGRAM ELEMENT NUMBER</b> 61102F	
<b>6. AUTHOR(S)</b> Jeffrey Brinker		<b>5d. PROJECT NUMBER</b>	
		<b>5e. TASK NUMBER</b>	
		<b>5f. WORK UNIT NUMBER</b>	
<b>7. PERFORMING ORGANIZATION NAME(S) AND ADDRESS(ES)</b> UNIVERSITY OF NEW MEXICO 1700 LOMAS BLVD NE ALBUQUERQUE, NM 87106 US		<b>8. PERFORMING ORGANIZATION REPORT NUMBER</b>	
<b>9. SPONSORING/MONITORING AGENCY NAME(S) AND ADDRESS(ES)</b> AF Office of Scientific Research 875 N. Randolph St. Room 3112 Arlington, VA 22203		<b>10. SPONSOR/MONITOR'S ACRONYM(S)</b> AFRL/AFOSR RTB2	
		<b>11. SPONSOR/MONITOR'S REPORT NUMBER(S)</b> AFRL-AFOSR-VA-TR-2017-0047	
<b>12. DISTRIBUTION/AVAILABILITY STATEMENT</b> A DISTRIBUTION UNLIMITED: PB Public Release			
<b>13. SUPPLEMENTARY NOTES</b>			
<b>14. ABSTRACT</b> Our bio-compatible and biomimetic research has been focused on the use of living cells, biomolecular interfaces and bio-mimetic processes to direct the formation of new classes of complex, symbiotic, hierarchical materials with life-like structure and functionality. This aim is predicated on two principal goals: 1) use of living/fixed cells to direct the formation of new classes of complex, hierarchical materials with lifelike (or new) structures and functionality, evidenced by the preservation of cell and organism structure in silica with sub 10-nm fidelity through a reaction with silicic acid, and transformation of these replicates to carbon or carbon/silica hybrids, enabling multiscale imaging without loss of resolution and 2) use of self-assembly to create engineered nano-to-microscale environments to direct new cellular behavior and confer enhanced biomolecular stability. These goals are premised on three key nano-to-microscale strategies pioneered by our team: silica cell replication (SCR), protocell platform for synthetic biology, cellular and biomolecular immobilization or stabilization using evaporation-induced self-assembly (EISA) and atomic layer deposition (ALD) and creation of biotic/abiotic interfaces through the interaction of rare earth oxides with bacterial membranes and metal organic framework (MOF) functionalization of mammalian cells			
<b>15. SUBJECT TERMS</b> silification			
<b>16. SECURITY CLASSIFICATION OF:</b>			

Standard Form 298 (Rev. 8/98)  
Prescribed by ANSI Std. Z39.18

DISTRIBUTION A: Distribution approved for public release.

<b>a. REPORT</b> Unclassified	<b>b. ABSTRACT</b> Unclassified	<b>c. THIS PAGE</b> Unclassified	<b>17. LIMITATION OF ABSTRACT</b>  UU	<b>18. NUMBER OF PAGES</b>	<b>19a. NAME OF RESPONSIBLE PERSON</b> ROACH, WILLIAM
					<b>19b. TELEPHONE NUMBER</b> <i>(Include area code)</i> 703-588-8302

# BIOCOMPATIBLE AND BIOMIMETIC SELF-ASSEMBLY OF FUNCTIONAL NANOSTRUCTURES

Final Report for Air Force Office of Scientific Research

Grant Number: FA9550-14-1-0066

Reporting Period: 1 February 2014 to 31 January 2017

**Principle Investigator(s):**

C. Jeffrey Brinker (PI) The University of New Mexico, 1001 University Blvd. SE Albuquerque, NM 87106, 505-272-7627, [cjbrink@sandia.gov](mailto:cjbrink@sandia.gov)

**Co-PI:** Darren Dunphy (co-PI) The University of New Mexico, 1001 University Blvd. SE Albuquerque, NM 87106, 505-272-7120, [ddunphy@unm.edu](mailto:ddunphy@unm.edu) (to Lumileds)

**Key Collaborators:** Jacob O. Agola PhD, Center for Micro-Engineered Materials, University of New Mexico, Albuquerque, NM 87131. Kimberly Butler PhD, Bioenergy and Defense Technologies Department, Sandia National Laboratories, Albuquerque, NM 87185. Rita Serda, PhD, Center for Micro-Engineered Materials, University of New Mexico, Albuquerque, NM 87131. Bryan J. Kaehr PhD, Advanced Materials Laboratory, Sandia National Laboratories, Albuquerque, NM 87185, and Department of Chemical and Nuclear Engineering, The University of New Mexico, Albuquerque, NM 87131. Jason C. Harper PhD, Bioenergy and Defense Technologies Department, Sandia National Laboratories, Albuquerque, NM 87185.

**Program Manager:**

Dr. William P. Roach  
Director (A), Math-Info-Life Sciences  
PM: NMS&E  
AFOSR/RTB2  
875 N. Randolph St  
Suite 325, Room 3112  
Arlington, VA 22203-1768  
DSN: 426-7722 Comm: (703) 588-8302  
FAX: (703) 696-7360  
[afosr.nature@us.af.mil](mailto:afosr.nature@us.af.mil)

## Table of Contents

<b>1.0 Overview</b>	<b>3</b>
<b>2.0 Brief Caption of Prior Accomplishments</b>	<b>5</b>
<b>3.0 Accomplishments: Last Three Years</b>	<b>5</b>
3.1. Understand Silica Cell replication (SCR)	6
3.2. Explore use of <i>protecell</i> platform for synthetic biology	13
3.3 Understand Cellular and biomolecular immobilization/stabilization	17
3.4 Understand biomimetic nanofabrication	21
3.5 Understand creation of biotic/abiotic interfaces and organisms	22
<b>4.0 Supporting Information for 1 February 2014 to 31 January 2017</b>	<b>37</b>
<b>4.1 Supported Personnel</b>	<b>37</b>
<b>4.2 Collaborators</b>	<b>38</b>
<b>4.3 Archival publications (published) during reporting period (acknowledge AFOSR support, full or partial):</b>	<b>39</b>
4.3.1 Published manuscripts	39
4.3.1 Refereed Publications in Preparation	41
<b>4.4 Other publications/presentations</b>	<b>41</b>
4.4.1 Books/Book Chapters	41
4.4.1 Invited Presentations	41
4.4.1 Contributed Presentations	42
<b>4.5 Awards / Honors / Service</b>	<b>42</b>
<b>4.6 Intellectual Property</b>	<b>44</b>
<b>4.7 Interactions/Transitions</b>	<b>47</b>
4.7.1 Biomolecular and Cellular Integration - Luna Innovations	47
4.7.2 Angstrom Thin Film Technologies LLC	47
4.7.2.1 Approach	48
4.7.2.2 Accomplishments	48
4.7.2.3 Impact	48
<b>5.0 References cited in the report.</b>	<b>48</b>

## 1.0 Overview

Over billions of years, natural materials systems have mastered the art of solving some of the most challenging engineering problems facing the modern world, e.g. energy harvesting, transduction and storage; water purification; self-sensing, repair and replication; simultaneously hard, tough, and strong protection systems. Natural materials exhibit well optimized property combinations that result from hierarchical designs characterized by structure and function on multiple scales, where the feature sizes are prioritized according to the relevant functional length scale (exciton, stress field, van der Waals contact, etc.). For decades, the elegance and functionality of natural materials along with their aqueous formation under ambient conditions have inspired diverse groups of scientists in attempts to mimic their designs and construction principles with the goal of imparting 'life-like' qualities to robust and manufacturable synthetic materials. Moreover, by employing the full spectrum of 'non-natural' chemistries, processing conditions, and fabrication tools now available, it has been anticipated that we could improve on Nature's designs and functions. To impart biofunctionality to manmade materials, much of recent research has focused on the incorporation of biomolecules with less focus on the incorporation of living organisms. Especially in areas like cell-based sensing, little effort has been made to engineer the physicochemical characteristics of the 3D bio/nano interface surrounding the cell. This is problematic in that cells are inherently sensitive to local nano-to-micro-scale patterns of chemistry and topography that together mediate chemical and mechanically induced signaling pathways and thus behavior. Furthermore, although it is recognized that biological components can direct the formation of robust 3D bio-composite materials as evident, for example, in siliceous marine organisms like sponges and diatoms, synthetic bio-mimetic processes have not yet achieved the elaborate hierarchical silica structures observed in nature. Finally, as materials scientists, we have largely failed to pursue compartmentalized materials designs and synthesis strategies that enable and exploit the development of chemical potential gradients both in the synthesis and 'operation' of biomimetic materials. The dynamic functionality evident in natural systems requires energy transfer and consumption and operation under conditions far from equilibrium. Synthesis of materials within scaffolded membrane bound compartments that enable directed energy and materials transfer could be a first step towards the formation of cell-like constructs (*protocells*) that could autonomously sense and respond to their external environments. Given these gaps, our research therefore sought to help overcome existing limitations of biomimetic design and processing. It exploited our numerous previous discoveries surrounding engineering of the bio/nano interface that had enabled the creation of several new materials classes and devices displaying a symbiotic relationship between the biotic and abiotic components. **First**, we discovered a generalized process, silica cell replication (SCR), wherein mammalian cells (as well as tissues and complete organisms) direct their exact replication in silica with preservation and protection of shape and many aspects of extra- and intracellular biofunctionality upon complete drying. The silica cell replicas preserve nm- to macro-scale cellular features and dimensions on both the cell surface and interior after drying at room temperature - and largely after calcination to 500°C. The process is self-limiting and self-healing, such that room temperature dried silica replicas can be hermitically sealed without any problem. Re-exposure of the SCRs to water

provides access to intracellular components, where evidence confirms preservation of biofunctional properties including cell surface antigens, receptor-ligand binding and enzymatic activities. **Second**, by fusion of lipid bilayer membranes on spherical nanoporous silica particles, we created a unique class of rudimentary cell-like constructs called *protocells* as fundamental tools for synthetic biology. These constructs provide a means for characterizing the dynamics and phase behavior of supported lipid bilayers on silica cell replicas or porous silica particles in a way that capture key aspects of natural cell systems. Compared to commonly used giant unilamellar vesicles, *protocells* offer several unique advantages: (1) as for natural cellular plasma membranes, the membrane bilayer of the protocell is supported on a porous, cytoskeleton-like scaffold through which the adhesion energy, stemming from hydrogen-bonding and electrostatic interactions, confers stability, lateral diffusivity and fusogenicity; (2) proteins and other membrane-bound components can be incorporated into the supported lipid bilayer (SLB) where they can diffuse and interact multivalently to achieve membrane-like functionality; (3) protocells can be easily loaded with nucleic acids, proteins, and messenger molecules to mimic the cytoplasm by simple immersion procedures. **Third**, we discovered the ability of living cells to direct the organization of extended nanostructures and nano-objects in a manner that creates a unique, conformal and highly biocompatible bio/nano interface that preserves aspects of biofunctionality after exposure to extreme conditions of desiccation, starvation, irradiation, and evacuation. Using amphiphilic phospholipids to direct inorganic self-assembly in the presence of living cells, we found that yeast, mammalian and bacterial cells can intervene to direct the self-assembly process to form a 3-dimensional interface at the cell surface which interfaces conformally and coherently with an ordered nanostructure. As an extension of this Cell-Directed Assembly (CDA) approach, we discovered a unique metabolically and optically controlled lithography approach Cell Directed Integration (CDI) that allows patterned integration of live cells into nominally solid-state devices. We observed that yeast, bacterial, and mammalian cells deposited on lipid/silica thin film mesophases catalyze the formation of a fully 3D bio/nano interface, preserving cellular function. Uniquely, both CDA and CDI allowed us to understand and direct cellular behavior in different ways (e.g. induced persister-like cellular states in confined yeast cells) by virtue of our ability to engineer the bio/nano interface. **Fourth**, we discovered different methods of creating biotic/abiotic interfaces through the interaction of rare earth oxides with bacterial membranes and functionalization of live mammalian cells with metal organic framework (MOFs). Through universal modification of bacterial organisms by rare earths, we established a new living biotic/abiotic phenotype with a unique combination of properties including insolubility, low toxicity, and optical activity following doping with optically active rare earth ions of Eu. Through MOF functionalization of mammalian cells, we established MOF induced spore-like hibernation state of live mammalian cells where MOF provides an exoskeletal protective coating which can prevent cell attachment and replication but allow transport of nutrients to ensure cell viability. Based on these findings, we believe that we have discovered important functional materials and revealed new functionalities and behaviors that can be important to sensing, energy harvesting, and adaptation to extreme environments of potential interest to the US Air Force.

**Significance** – Work supported by AFOSR over the past three years has allowed us to use biomolecular-interfaces and bio-mimetic processes to create new classes of complex, symbiotic, hierarchical materials with life-like structure and functionality. These achievements have been registered in the areas of silica cell replication (SCR), *protocell* platform for synthetic biology, cellular and biomolecular immobilization and creation of biotic/abiotic interfaces using rare earth oxides and metal organic frameworks (MOFs). By introducing natural, non-native, and even inorganic materials into these interfaces, we have created hybrid materials capable of tailorable complex functions and impart new non-native behaviors – like extremophile characteristics. These materials, representing the integration of biological functionality into nano- and micro- scale systems, have a wide range of uses, including: cell-based sensing in extreme environments; new, sensitive cellular interrogation and imaging systems; general platforms for cargo delivery in complex cellular environments, understanding and exploiting cell-cell communication including disease, injury, and therapy; and the creation of “living materials” with new phenotypes that could sense and respond to their environment through the integration of individual organisms or cellular populations into defined platforms and systems.

## **2.0 Brief Caption of Prior Accomplishments**

Nature’s solutions to achieving highly functional materials often involve multiple, disparate components (hard/soft or hydrophilic/hydrophobic) combined in 3D hierarchical architectures resulting in synergistic, optimized properties and combinations of properties. Emulating such proven natural designs in robust engineering materials using efficient, manufacturable processing approaches still remains a major challenge to materials science and engineering. The important research support we have consistently received from the AFOSR over the past several years has enabled us register high impact accomplishments characterized by discovery of numerous self-assembly materials, living cell-directed assembly platforms for understanding/studying living cells under controlled and confined conditions, biotic/abiotic materials with optimized properties and/or complex functionalities among others. Representative examples include; discovery of living nanocomposites in which live bacterial and yeast (*Saccharomyces cerevisiae*) cells are encapsulated into ordered silica matrices that allow us to understand their physiological and metabolic response at genome level<sup>1</sup>, silicified cell replicas with preserved shape and biofunctionality<sup>2</sup>, rudimentary cell-like constructs (protocells) composed of nanoporous particles encapsulated within a supported lipid bilayer<sup>3-5</sup>, silica bioreplicated whole organism with preserved shape and features<sup>6</sup>, generalized atomic layer deposition (ALD) synthesis platform capable of preparing any arbitrary peptide membranes<sup>7</sup>, universal rare earth (RE) modified bacterial phenotypes with the potential to confer extremophile-like properties, serve as an RE biomining platform and inhibitor of metal surface corrosion. These discoveries have provided a fundamental understanding of living-cells in ways rarely known before. A summary of the accomplishments registered during the past three years is provided in the following sections.

## **3.0 Accomplishments: Last Three Years**

In the following sections we describe objectives and findings of Grant # FA9550-14-1-0066 conducted and published during the period: 1 February 2014 to 31 January 2017.

### 3.1. Understand Silica Cell replication (SCR)

**Finding 1:** Confirmed the chemistry of silicification process and also demonstrated that silicification preserves different kinds of cellular features in biological interfaces consistent with the water replacement theory.

**Specifics:** We pioneered the replication of cells, tissues, and organisms in hybrid silica biocomposites, along with their further transformation to refractory and robust silica and carbon hierarchical materials. This simple procedure relies on the deposition of silica in the form of molecular silicic acid ( $\text{Si}(\text{OH})_4$ ) onto fixed biological interfaces under mildly acidic (pH 3) conditions where self-condensation is suppressed. The procedure preserves macro- and nanostructure surfaces to a resolution of less than 10 nm in  $\text{SiO}_2$  (after calcination in air) or conductive carbon (after pyrolysis in argon at  $1000^\circ\text{C}$  followed by dissolution of the inorganic framework). To be able to explain the silica replication procedure, we had hypothesized that, silicic acid could replace/displace hydrogen-bonded interfacial water at cellular/biomolecular interfaces and be concentrated and catalyzed amphoterically by proximal membrane that stop when catalytic proteinaceous silica condensation sites are occluded. This hypothesis was premised on the fact that both water and silicic acid can form extended tetrahedrally coordinated H-bonded networks. To examine this hypothesis in more detail, we carried out metadynamic simulations using  $\text{Si}(\text{OH})_4$  force field and an atomistic model of a POPC bilayer of  $\text{Si}(\text{OH})_4$  and  $\text{H}_2\text{O}$  diffusion through a lipid bilayer (**Figure 1A**). This was done in parallel with spectroscopic characterizations including FTIR, Raman scattering, and NMR. From in situ FTIR analysis of adherent mammalian cells fixed to a germanium 10-bounce ATR plate and then subjected to silicification process with 0.1 M tetramethylorthosilicate (TMOS) at pH 3, we confirmed an initial rapid initiation of silica formation followed by a longer phase of slower deposition, consistent with a self-limiting reaction process (**Figure 1B**). Other FTIR analyses indicated that the chemical structure of the cellular protein scaffold is preserved in this reaction, with NME data confirming that the reaction is driven by the presence of the biomolecular interface. In addition to elucidating the chemistry of silicification process, we demonstrated preservation of different kinds of cellular features in these biological interfaces in consistent with the water replacement theory. We elucidated that, the shape and features of complete intact silica-replicated/reinforced organisms are preserved by silicification during their drying, calcination and transformation, thereby enabling sectioning (e.g. FIB) and imaging across the macro- to nanoscale without any loss of resolution due to charge induced specimen damage or imaging artifacts (**Figure 2**).

We also demonstrated that carbon replication of organs and tissues can enable dissection *ad infinitum* and SEM imaging of these interfaces without conductive coatings, while preserving 3D structural context, where the several-nm thick silica shell serves as a stabilizing scaffold maintaining multicellular structure to a temperature of 1000° C (**Figure 3A.**) Using Raman scattering technique, we showed that in the carbon replicated chicken embryo's heart, carbon is present as microcrystalline graphite with a significant amorphous C content in these organs and tissues (**Figure 3B.**)

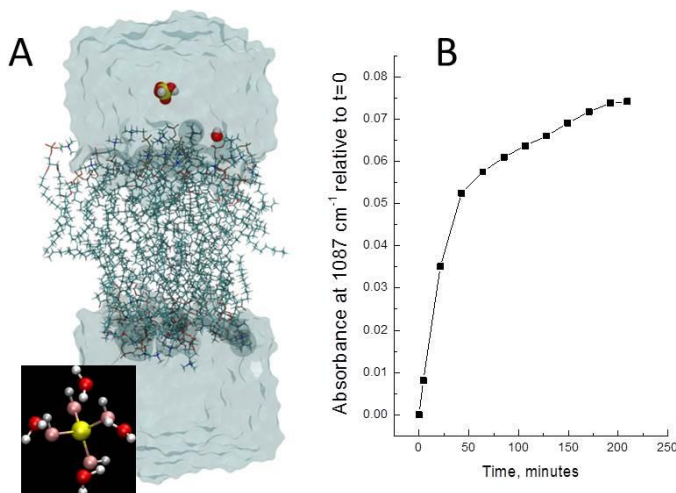


**Figure 1.** A) Snapshot of metadynamic simulations of  $\text{Si(OH)}_4$  and  $\text{H}_2\text{O}$  diffusion through an atomistic POPC bilayer (inset shows detail of H-bonded model of  $\text{Si(OH)}_4$ ) (Lucio Ciacchi, Bremen), B) In situ Ge ATR FTIR data of the Si-O band intensity for fixed cells undergoing silicification.

Consistent with the preservation of shape and features of silica replicated biological interfaces, we addressed the question of whether biofunctional characteristics of these interfaces were also preserved. Four strategies including antibody labeling, receptor-ligand binding, cell-cell communication and intracellular enzymatic activities were used to address this important question. Through antibody labeling of surface antigen (epidermal growth factor receptor, EGFR), we demonstrated formation of silica mesh on the cell membrane by showing that, during the initial stages of silicification, EGFR remains accessible to the antibody, however, after 22 hours of silicification, silica uniformly obscures all access to EGFR receptor and prevents antibody binding (**Figure 4**). Removal of ca. 7 nm of silica using buffered hydrofluoric (HF) acid then ensured that antibody binding to EGFR became

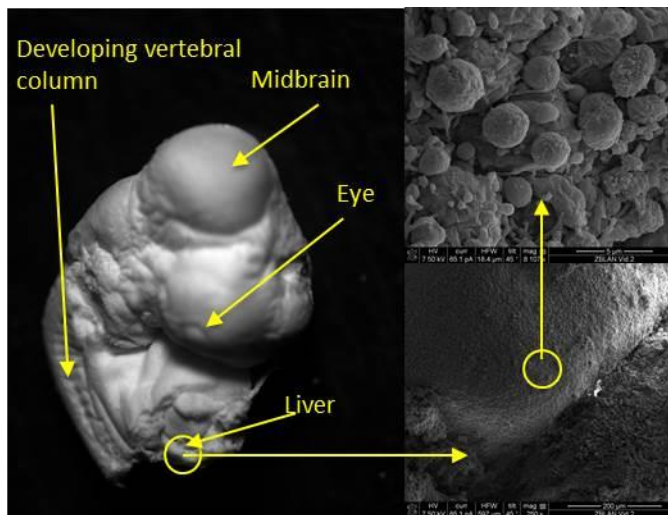


**Figure 2.** Multiscale optical/SEM imaging of silicified chicken embryo,

identical to that of the as-fixed (pre-silicified) state (**Figure 4**), confirming evidence of silica obscuration. We then determined the preservation of membrane and organelle interface features by labeling A549 cells with different kinds of probes (anti-EGFR antibody, 150kDa, 3.5 nm; anti-Lamp-1 antibody, 120 kDa, 3.3 nm; anti-Cox IV antibody, 17 kDa, 1.7 nm; and Hoechst nucleus dye, 0.5kDa, 0.5 nm) before silicification followed by sample imaging after each silicification step. Evidently, even after the silicification process, antibody access to cellular antigens was still maintained (**Figure 5**), however, after drying of silicified cells to generate silica network/mesh, only the small molecule Hoechst dye was able to access the cell interior (nucleus) possibly due to the reduction of the intrinsic pore size of the dehydrated silica mesh upon elimination of water molecules via drying. Thus, removal of silica layer restored access to the internal structure of the A549 cells with successful antibody staining of the desilicified cells conclusively demonstrating preservation of biochemical features through silicification process.

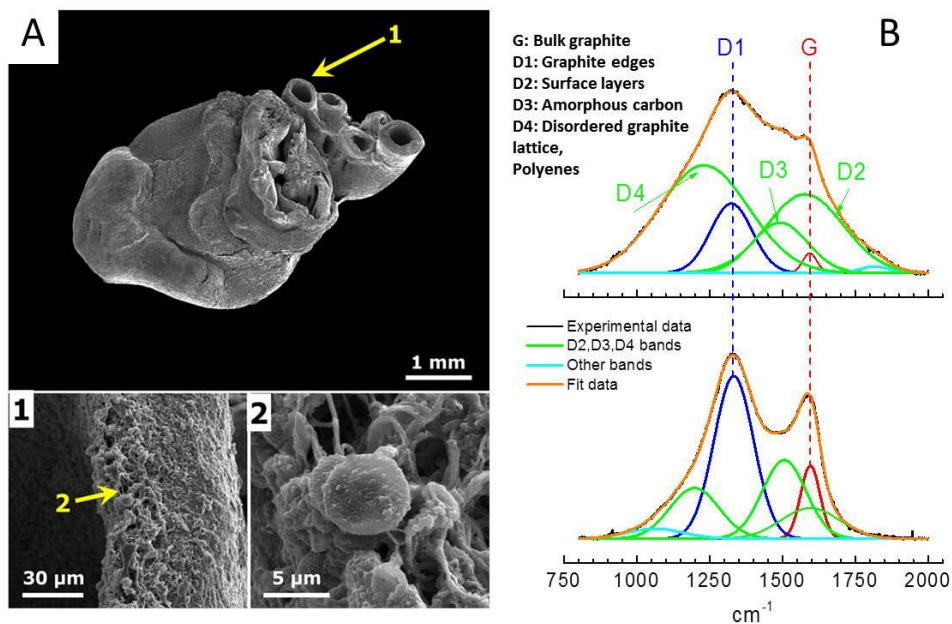


**Figure 3. A)** Carbon replica of chicken embryo's heart, and **B)** Raman spectra (785 nm excitation) of carbonized heart, before (top) and after (bottom) removal of  $\text{SiO}_2$ . Data is consistent with the presence of microcrystalline/ amorphous carbon.

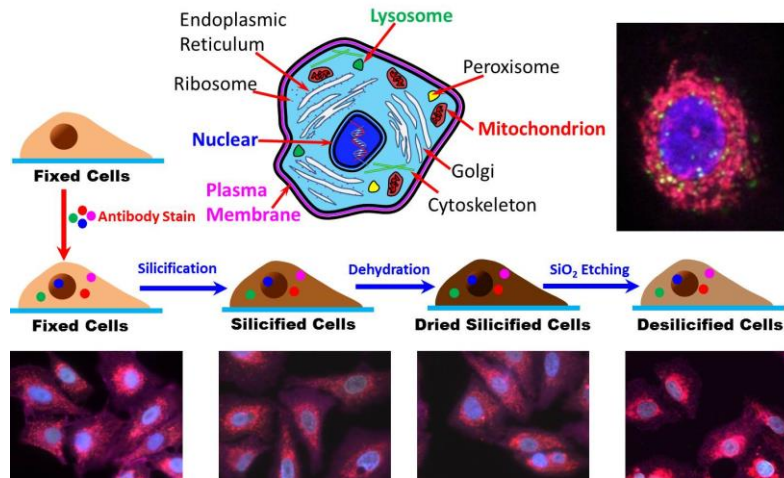


**Figure 4.** Confocal microscopy images of A549 cell stained with Anti-EGFR (magenta), Lamp-1 (green), Cox IV (red) antibodies, and Hoechst (blue) dye for the nucleus before silicification, drying, and desilicification. Evidence confirms preservation of biochemical features.

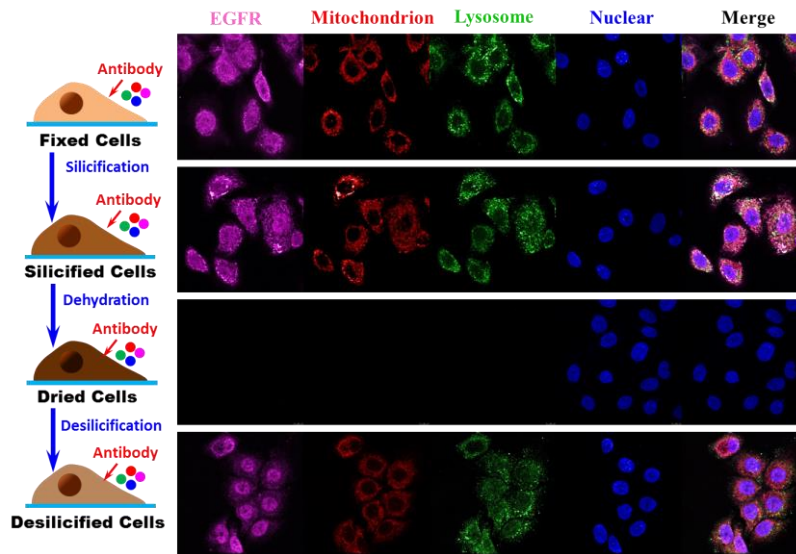


**Figure 5.** Confocal images of A549 cell plasma membrane and organelles stained with Anti-EGFR (magenta), Lamp-1 (green), Cox IV (red), and Hoechst (blue) probes after silicification, drying, or desilicification, showing reduced internal access after drying due to the reduction of silica pore size.

Further evidence of the preservation of surface antigens in silicified cells was also obtained from the interactions of live A549 cells with silicified/desilicified A549 cells (**Figure 6**). Through light microscopy imaging, live A549 cells (in suspension) displayed absolutely no interaction with the adherent silicified A549 cells (**Figure 6A**), however,

after etching of the silica layer with buffered HF acid solution, surface antigens were re-exposed and the desilicified A549 cells then exhibited increased interactions with the live A549 cells, suggestive of the protection or preservation of the surface antigens through silicification (**Figure 6B**).

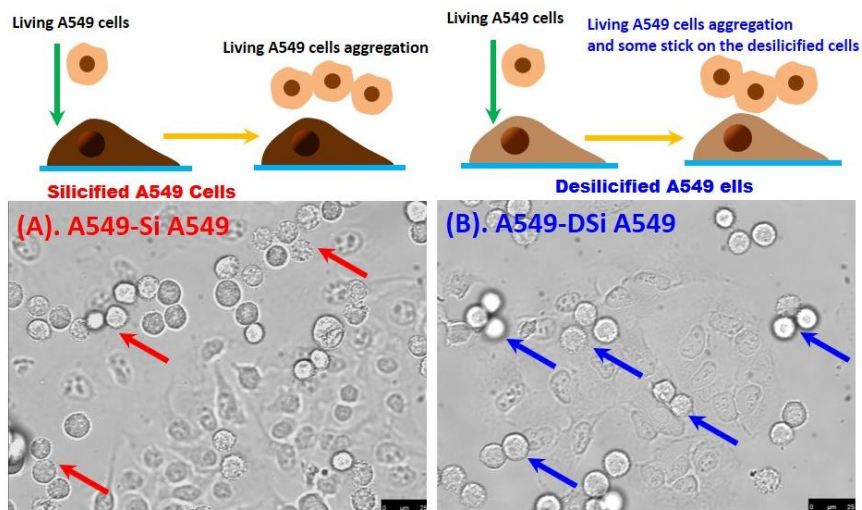


**Figure 6.** **A).** Wide field microscopy image showing lack of interaction between live A549 cells and silicified adherent A549 cells (red arrows), and **B).** Wide field microscopy image showing evidence of interaction between live A549 cells and ‘desilicified’ adherent A549 cells (blue arrows). Desilicification exposes surface antigens and leads to cell to cell recognition.

Consistent with the preservation of the surface antigens, we assessed the activities of multiple classes of intracellular enzymes in silicified cells to understand if biofunctional characteristics were also preserved. HeLa cells were silicified and then stored for at least one week before assessing the enzymatic activity. As a representative example, we demonstrated that the activities of acid (cytoplasmic) and alkaline (membrane-associated) phosphatases were differentially preserved between one week and one month of sample storage after silicification (**Figure 7A-D**). Significantly, we noted that cell silicification was able to rescue the high instability of membrane associated alkaline phosphatase relative to the acid phosphatase enzyme. Taken together, all these findings confirmed the utility of silicification to preserve the integrity of the biomolecular components of the cell alongside their intrinsic characteristics.

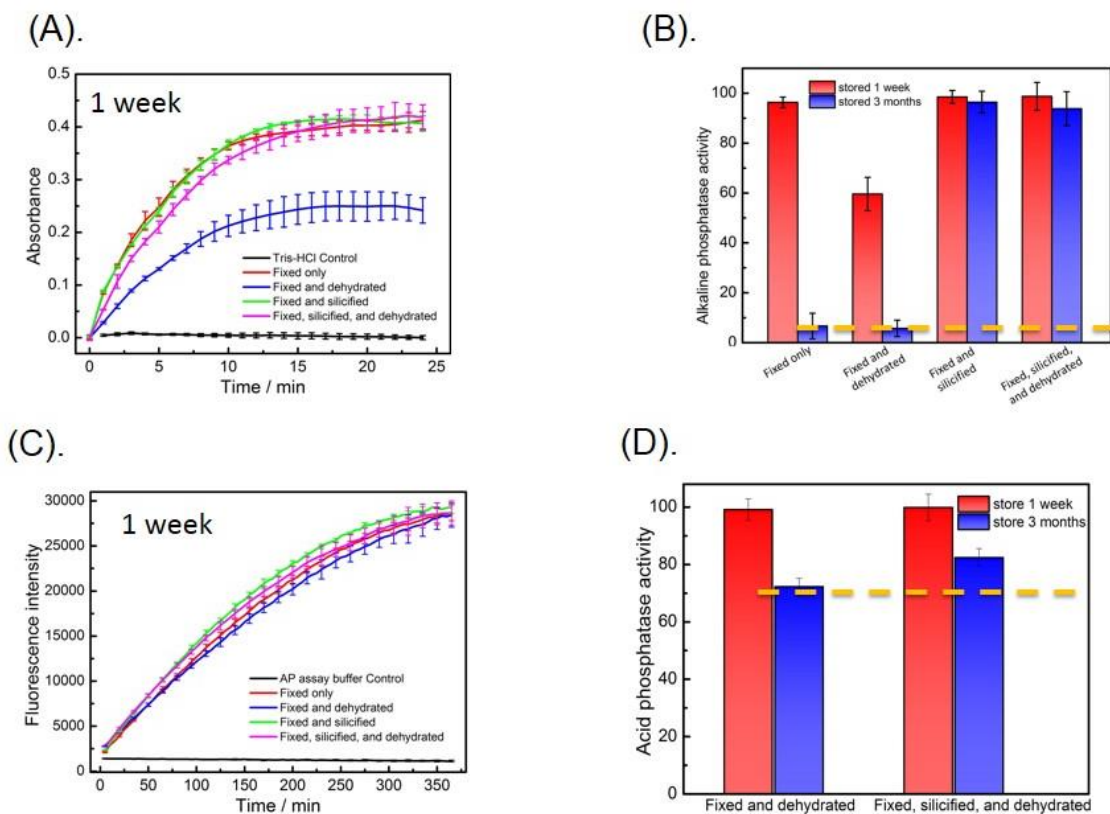


**Figure 7.** **A).** Activity of alkaline phosphatase (ALP) enzyme (membrane associated) in silicified HeLa cells stored for one week; **B).** Comparative ALP activity in silicified HeLa cells stored for one week versus three weeks; **C).** Activity of acid phosphatase (AP) enzyme (cytoplasmic distributed) in silicified HeLa cells stored for one week and, **D).** Comparative AP activity in silicified HeLa cells stored for one week versus three weeks.

Another important aspect of silicified cells we elucidated dealt with their mechanical properties. Through our collaborator at Nanyang University in Singapore, we used nanindentation technique to assess the mechanical characteristics of silicified A549 and HeLa cells. Distinct and consistent cell-specific and processing-dependent behaviors, associated with complex deformation patterns were observed (**Figure 8A-D**). Despite complex deformation pathway, we confirmed consistent right shifted load-displacement curves that varied progressively with the silicification process.

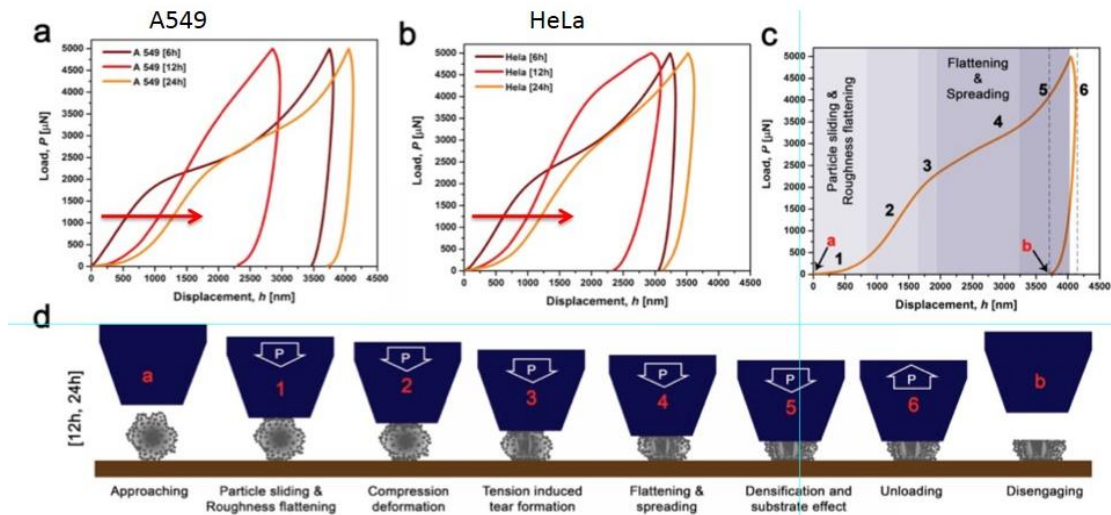


**Figure 8.** A). Nanoindentation curves of A549 cells at increasing silicification times; B). Nanoindentation curves of HeLa cells at increasing silicification times; C). Structural changes of silicified A549 cells during nanoindentation process and, D). Schematic description of the nanoindentation process.

**Finding 2:** Confirmed ability of silicification to stabilize bacterial surface morphology by reinforcing the bacterial membrane, resulting in stimulation of macrophage Raw264.7 cells.

**Specifics:** Based on our notable work on silica replication of mammalian cells, we sought to elucidate silica replication of bacterial cells using the same principle of depositing silica in the form of molecular silicic acid ( $\text{Si}(\text{OH})_4$ ) onto glutaraldehyde fixed bacterial cell surface under mildly acidic (pH 3) conditions. Using model *Salmonella typhimurium* LT2, we investigated the effect of bacterial silicification on the interactions of *Salmonella typhimurium* LT2 cells with live mammalian mouse macrophage Raw264.7 cells. We confirmed that silicification could stabilize bacterial surface morphology by reinforcing the bacterial membrane (**Figure 9A**), and this stimulated interactions with and uptake by Raw 264.7 cells (**Figure 9B**). *Salmonella typhimurium* LT2 being Gram-negative bacteria with immune active pathogen-associated molecular patterns (PAMPs) such as lipopolysaccharide (LPS) on the membrane, we hypothesized that these molecules were not perturbed by silica layer on the membrane and therefore could still stimulate macrophage cells. Using these findings, we are now exploring how we can use silicified bacterial cells to develop a stable ‘zombie’ vaccine platform with adjuvant properties.

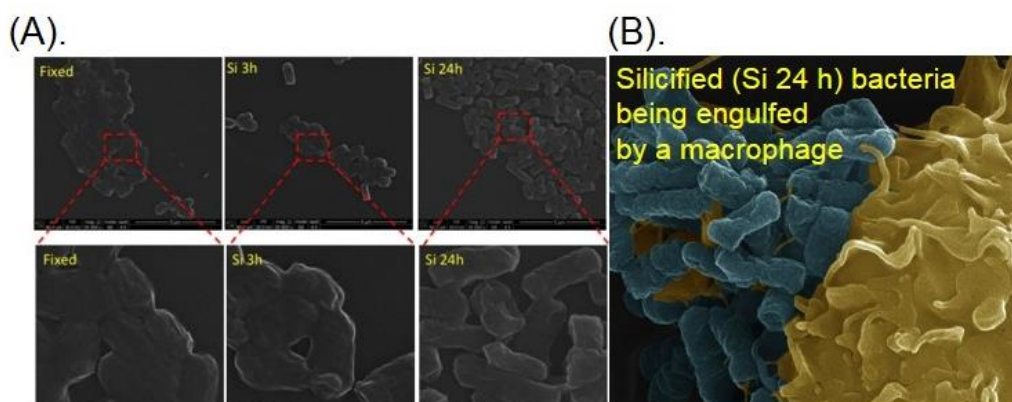


**Figure 9.** Scanning electron microscopy (SEM) image of: **A).** Silicified *Salmonella typhi*. *LT2* cells. Silicification preserves the overall bacterial cell morphology, as evidenced by the 24 hour treated bacteria (Si 24h) compared to fixed only cells, and **B).** The pseudo-colored mouse macrophage Raw264.7 cell (yellow) is captured in the process of internalizing a cluster of silicified bacteria cells (blue; 1 h co-incubation at 37 °C). The macrophage cell membrane is expanded outward to engulf bacterial cell consistent with phagocytosis.

### 3.2. Explore use of *protecell* platform for synthetic biology

**Finding 1:** Used combined tools of fluorescence recovery after photo-bleaching, fluorescence correlation spectroscopy, NMR fluorescence, fluorescence resonance energy transfer (FRET) and wide field microscopy to demonstrate the effect of the nanoporous silica support on the *protecell* platform and the utility of the *protecell* platform to mimic the unique characteristics of the native red blood cells (RBCs).

**Specifics:** Using our highly configurable '*protecell*' platform, comprised of lipid bilayers fused onto 3D porous silica scaffolds (mesoporous silica cores of ca. 25-250 nm diameter, or silica replicas of intact cells, **Figure 10A**), we sought to recapitulate minimalist cellular function to create synthetic cell models that could replicate two important aspects of natural membrane structure: support on 3D scaffolds and curvature dependent dynamics and phase behavior. Although biophysical properties of cell-mimetic membrane compositions have been studied for decades as Giant Unilamellar Vesicles (GUVs), GUVs still lack both of these critical features. To this end, using fluorescence recovery after photo-bleaching, fluorescence correlation spectroscopy, NMR, etc., we carried out the first experiments of the dynamics and phase behavior of lipid bilayers supported on biomimetic 3D scaffolds. Our results revealed that, in this configuration, the nanoporous

silica support suppresses both the lipid melting temperature and macroscopic lipid diffusion rate possibly through suppression of the water ‘buffer’ layer normally present between the lipid and substrate in supported bilayers. This unusual dynamics and phase behavior indicated a non-uniformity of the bilayer due to curvature differences along the membrane (**Figure 10B**). Also, by incorporation of a FRET-based protein biosensor and enzyme within SCRs, we confirmed 3D confinement within the molecularly crowded silica cell replica. This confinement modified biomolecular activity in a manner similar to confined living cells.

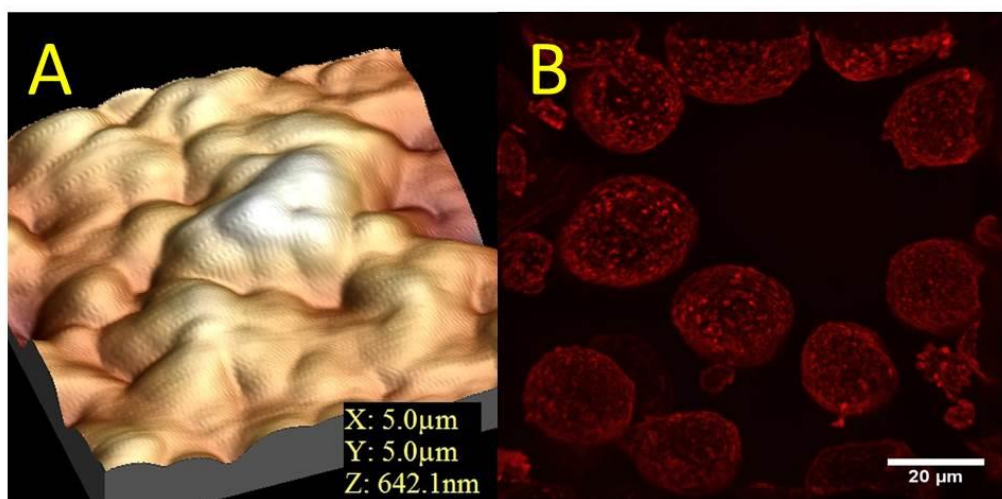


**Figure 10.** **A)** Atomic force microscopy (AFM) image of conformal supported lipid bilayer fused onto a SCR, and **B)** 3D reconstruction from fluorescence microscopy of SCRs coated with raft-forming lipid bilayers doped with rhodamine labels that associate with the raft phase, showing curvature-dependent non uniformity of the membrane (image courtesy of Viviane Ngassam, Parikh Group, UC Davis).

We expanded our studies of supported lipid bilayers to *protocell* constructs produced by the fusion of natural cellular membranes onto silicified cellular cores. This construct has the distinct advantage of containing cell membrane proteins whose functionality or lack thereof can be investigated upon generating the *protocell* platform. Z-stack confocal images of these particles coated with lipid bilayers doped with rhodamine showed non-uniform curvature-dependent lipid bilayer coverage (**Figure 11A-C**), as was previously seen for synthetic bilayers reconstructed onto silicified cells. Fluorescence recovery after photobleaching (FRAP) and antibody labeling confirmed the reconstitution of lateral fluidity in these natural membranes and the preservation of biochemical features after membrane fusion onto silicified cores respectively (**Figure 11**). Taking advantage of the *protocell* platform produced by the fusion of natural cellular membranes onto silicified HeLa cell cores, we mimicked the unique characteristics of red blood cells (RBCs) and rebuilt RBC constructs that can maintain the natural curvature of RBCs and also achieve/ensure circulation in the blood vessels of the Ex-Ovo chicken embryo (CAM). Using silica cell replication combined with layer-by-layer assembly and vesicle fusion, we

confirmed that our rebuilt RBC could maintain the natural biconcave shape of native RBCs after silica etching and native RBC ghost vesicle fusion steps (**Figure 12A-D**).

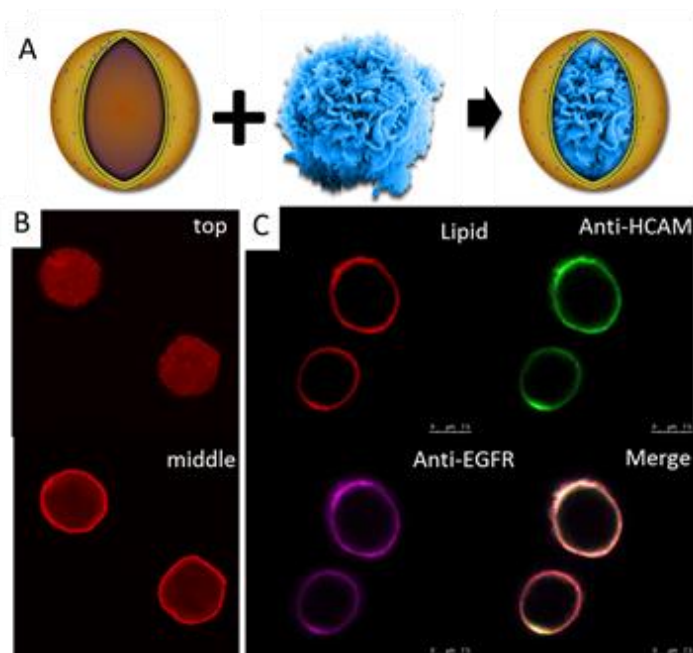


**Figure 11.** A). Schematic representing the formation of 'protocell' platform B). Confocal microscopy images of lipid bilayer (red) coating on HeLa cell silica replica (top is top slide, bottom is middle slide) C). Confocal microscopy images of native HeLa cell membrane liposome (red) coating on HeLa cell silica replica stained with Anti-EGFR antibody (magenta) and Anti-HCAM antibody (green).

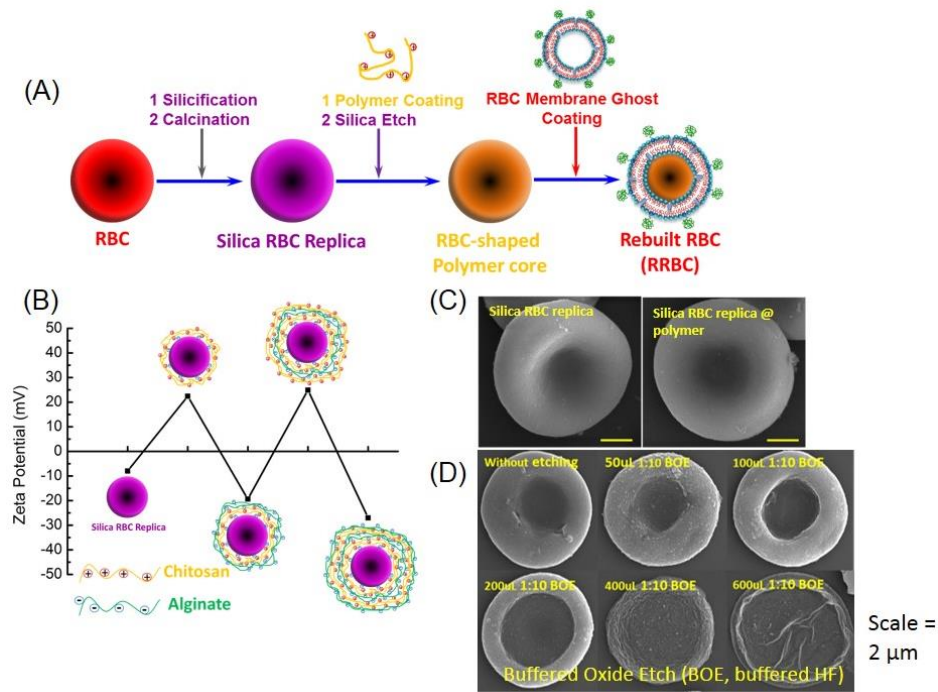


**Figure 12.** A). Schematic of rebuilding artificial and functionalized red blood cells; B). Zeta potential measurements during layer by layer assembly process; C). Scanning electron microscopy (SEM) images of silica red blood cell replica and silica red blood cell replica with polymer core (Si-RBC @polymer), and D). Si-RBC @polymer during etch process to form Polymer-RBC.

Significantly, while the rebuilt RBC was able to easily circulate in the deep blood vessels of the Ex-Ovo chicken embryo (CAM), both the RBC-shaped polymer cores and Si-RBC+polymer@RBC ghosts could not exhibit that characteristic because they got arrested in the CAM capillary bed (**Figure 13 A-F**), testifying that with good bioengineering improvements, the rebuilt RBC can be a versatile delivery platform for cargos such as hemoglobin. We are now exploring how to design and improve rebuilt RBCs that can be loaded with hemoglobin and/or other small molecule therapeutics.

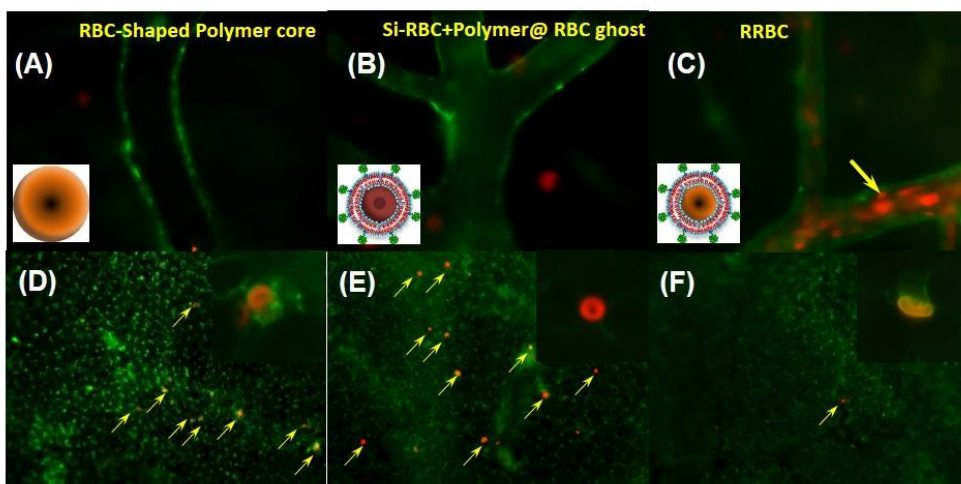


**Figure 13.** Fluorescence image of: **A)** RBC-shaped polymer core; **B)** Si-RBC@polymer and RBC ghost and **C)** RRBC within the chicken embryo deep blood vessel. An inset of fluorescence image of: **D)** RBC-shaped polymer core, **E)** Si-RBC@polymer and RBC ghost, and **F)** RRBC within the chicken embryo capillary bed.

### 3.3 Understand Cellular and biomolecular immobilization/stabilization

**Finding:** Confirmed that encapsulation of yeast and bacterial cells in silica matrices induces changes at the genome level giving rise to ‘*persister-like*’ cellular states in yeast cells and preservation of the biofunctionalities of the encapsulated bacterial cells. Based on, evaporation-induced self-assembly (EISA) combined with atomic layer deposition (ALD), developed a revolutionary method of trapping carbon dioxide (CO<sub>2</sub>) using carbonic anhydrase enzyme.

**Specifics:** Unicellular organisms such as yeast respond to changing conditions in their external environmental by promptly adapting internal cellular functions through reorganization of genomic expression patterns/profiles. Although microarray studies have been used to measure yeast genomic expression in culture, yeast embedded in biofilms, where some cells exist in a “*persister state*” which is thought to be important for microbial resistance, have not been examined before using the same approach. We carried out the first genome wide, longitudinal evaluation of confinement induced behavioral changes of yeast (*S. cerevisiae*) cells encapsulated by; cell-directed assembly (CDA) within a phospholipid/silica film, physical entrapment in a glycerol/silica gel, and spray drying based entrapment within a phospholipid/silica matrix. Affymetrix™ microarray technology was used to measure the yeast genomic expression, and functional analysis was performed using the Database for Annotation, Visualization, and Integrated Discovery (DAVID) to find the enriched or over-represented Gene Ontology (GO) categories among the differentially expressed genes. For all the three methods of encapsulation, we

confirmed cellular behaviors consistent with induction of 'persister-like' cellular states, with each encapsulation method resulting in a unique gene expression pattern (Figure 14). The gene expression patterns revealed by our DAVID analysis were consistent with the properties of persister cells, with down regulation of genes responsible for transport across the plasma membrane, transcription, translocation, and ribosomal processing, against up regulation of genes responsible for stress response, cell catabolic, and autophagic processes.

Through gene chip analysis, we established a correlation

between gene expression and the corresponding distinct metabolic states induced in *S. cerevisiae* from each encapsulation method (Figure 15.)

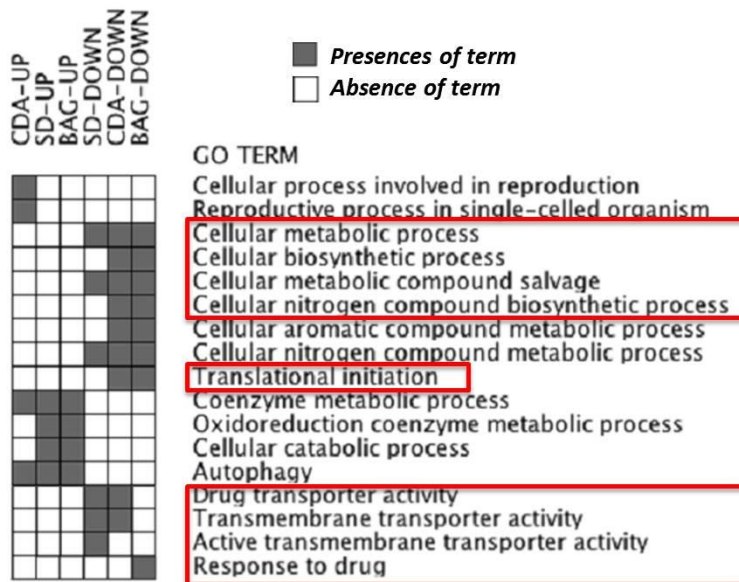


**Figure 14.** Gene expression heat map for yeast immobilized by CDA, within a silica/glycerol gel (BAG), or by spray drying with lipid and silica (SD), showing patterns of gene up- and down-regulation.

These observations led us to hypothesize that the encapsulation procedures induced and/or selected for a single species population of persister cells by mimicking some of the environmental features of biofilm formation. We believe that these findings could prove to be an invaluable tool for analyzing these cells and potentially improve the ability to combat antibiotic resistance and fungal infections.

In a related way, we assessed encapsulation of bacterial cells in silica based matrices through the process of cell-directed assembly (CDA), interfaced with scalable spray drying technique which enables large-scale production of functional nano-biocomposites (NBCs) containing living cells within ordered 3D

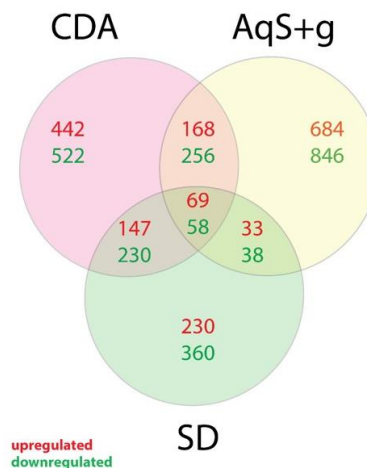


**Figure 15. A).** Distribution of all differentially expressed genes from *S. cerevisiae* cells encapsulated within three differing silica matrices: Cell-directed assembly (CDA); spray drying (SD); aqueous silicate with glycerol (AqS+g).

lipid-silica nanostructures (**Figure 16A-G**). In CDA, cell functionality and accessibility are preserved in a nominally dry, “solid-state” miniaturized sensor without the need for an external fluidic system. The process is aided by amphiphilic short-chain lipids that serve as structure directing agents to organize hydrophilic silicic acid precursors into highly ordered periodic lipid-silica mesophases. In this framework, we established that the spray-dried NBC materials are mechanically robust, with controlled structures spanning the nanoscale to microscale sizes depending on spray-drying conditions (**Figure 16A-G**). The biofunctionality of NBC-encapsulated bacterial cells was found to be preserved for months, as confirmed by intracellular adenosine triphosphate (ATP) levels in encapsulated *E. coli* bacterial cells (**Figure 17**).

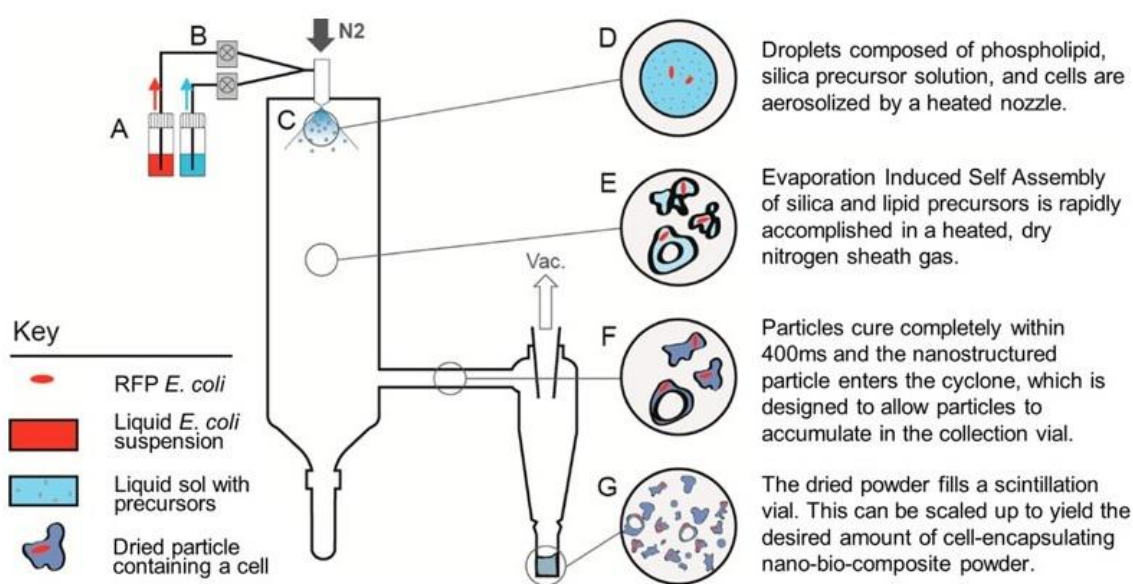


**Figure 16.** Schematic of the spray-drying process using a Büchi B-290 mini spray drier for the production of lipid-silica NBCs. Solutions of cells in liquid suspension and lipid-silica precursors are mixed in scintillation vials (**A**) and dispensed into the sprayer nozzle via peristaltic pumps; (**B**). This mixture is aerosolized by the heated nozzle in a sheath of N<sub>2</sub> gas (**C**). Droplets (~10-100 μm diameter) consist of cell and lipid (**D**). The droplet size can be varied by changing the ratio of the N<sub>2</sub> gas flow rate to that of the liquid feed rate. (**E**) Lipids organize silica precursors into an ordered nanostructure as the solvent evaporates during EISA. (**G**) Particles are fully dried before entering the cyclone (**F**) and flow through the cyclone vortex into the collection chamber.

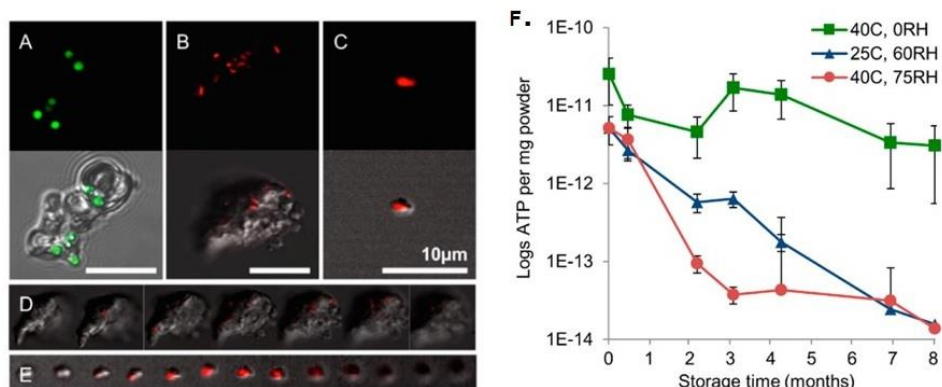


**Figure 17.** Confocal microscopy images of NBCs; **A)** Green fluorescent latex beads of 1  $\mu\text{m}$  used to provide a baseline for spray-dried particles. Encapsulated red fluorescent beads are observed in collapsed merged z-stack images of a typical large, **B)** and small (**C)** particle. Particles are shown to fully encapsulate cells as confirmed with three-dimensional z-stack sectioning of the same large **D)** and small **E)** and **F)**. ATP-based viability assay of aged NBCs confirming that encapsulated cells are viable for >8 months with less than  $1\text{-log}_{10}$  loss in ATP for samples stored at 40  $^{\circ}\text{C}$  and 0% relative humidity (RH). The confocal images demonstrate discrete, spray-dried particles that fully encapsulate cells or cell surrogates and ATP say also demonstrates that the long-term viability.

In our further understanding of biomolecular immobilization strategies, we used evaporation-induced self-assembly (EISA) combined with atomic layer deposition (ALD) and constructed a 10-nm thick hydrophilic membrane composed of ordered 6-nm diameter hydrophilic pores for the confinement of carbonic anhydrase (CA) enzyme within an ultra-thin nanostructure-stabilized biomimetic membrane for  $\text{CO}_2$  separation (**Figure 18**). To fabricate this membrane structure, a nanoporous silica film was deposited in a porous alumina substrate using EISA. ALD modification with hexamethyldisilazane was then used to introduce hydrophobic  $-\text{CH}_3$  groups throughout the internal surface of the film. Subsequent processing of the top surface by oxygen plasma removed a thin layer of the  $-\text{CH}_3$  modification, reestablishing hydrophilic  $\text{Si-OH}$  along the pore channel surface to a depth controlled by the plasma dose. Carbonic anhydrase was then added by soaking from an aqueous solution and localized within a liquid layer in the hydrophilic portion of the membrane. This increased the rate of interconversion between  $\text{CO}_2$  and  $\text{H}_2\text{CO}_3$  by a factor of  $10^7$ . Transport across the membrane, driven by a  $\text{CO}_2$  pressure gradient was found to be much faster than in conventional solid state  $\text{CO}_2$  separation membranes due to the thinness of the liquid layer and increased diffusion rates through liquids in comparison to solid membranes. In this nanoscale confined state of CA, we measured  $\text{CO}_2$  permeability and  $\text{CO}_2/\text{N}_2$  selectivity across this membrane, and found 3x faster permeation rate, 20x higher  $\text{CO}_2/\text{Ar}$  selectivity, and 7x lower fabrication cost when

compared to polymeric membranes, with increased stability over a wide temperature range (0-60° C) and time period (> 2 months). Additionally, corresponding molecular dynamics-based simulations revealed that this confined state resulted in greatly enhanced rotational velocity with this faster rotation likely increasing the apparent rates of both the forward and backward reactions, suggesting a new mechanism for enhanced enzymatic activity.

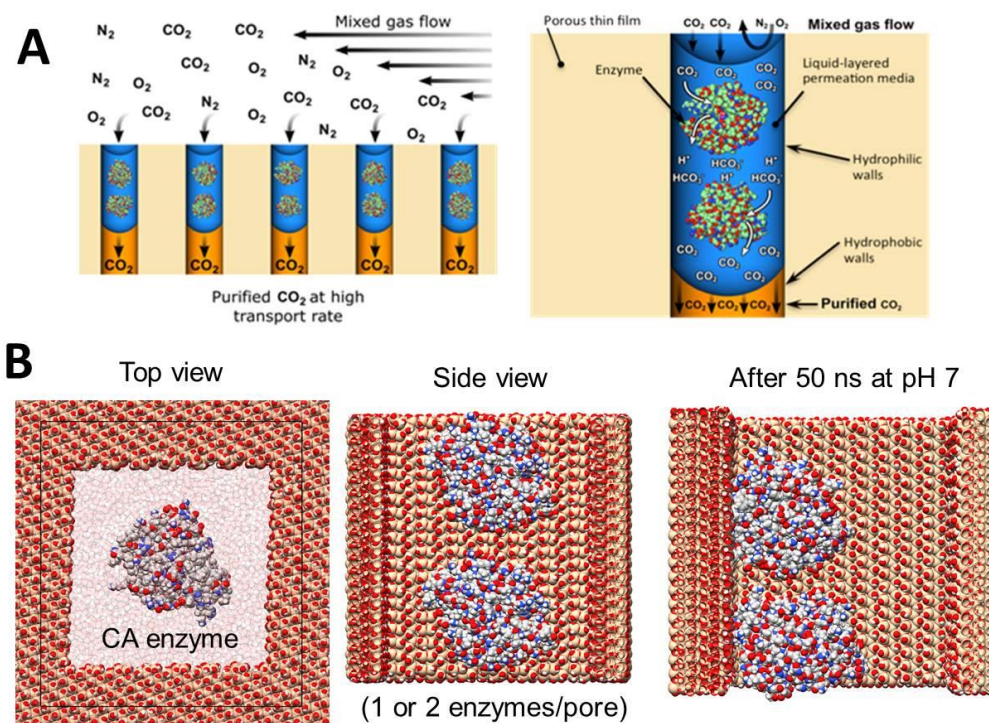


**Figure 18.** A) Schematic of the enzymatic CO<sub>2</sub> membrane, B) Atomistic simulation box (left two images) plus results (right image) after 50 ns showing interaction of the enzyme with the silica nanopore wall, stabilizing the enzyme against aggregation.

### 3.4 Understand biomimetic nanofabrication

**Finding:** Used plasma-directed molecular layer deposition process to develop biomimetic water separation membrane with the dimensional scale and complexity of natural membranes.

**Specifics:** Natural ion and molecular channels possess high flux and near perfect selectivity, due to pore size asymmetry and shape as well as stratified, non-uniform pore surface chemistries stretching to nanometer length scales. This presents difficulties with respect to using conventional routes to synthesize man-made synthetic polymeric or inorganic membranes from these channels. To enable fabrication of asymmetric

structures with the dimensional scale and complexity of natural membranes, we pursued a plasma-directed molecular layer deposition process to fabricate a several nm-thick biomimetic water separation membrane. Amide polymerization on the surface of a nanoporous support prepared by EISA, which produces membranes with remarkable salt rejection (90%) and water flux (3x) when compared to conventional commercial polymer membranes was used. We used a generalized ALD synthesis procedure to prepare arbitrary peptide membranes, where systematic alteration of the peptide residue ‘R’ allows for control of charge, hydrogen bonding, and hydrophobicity. This process uses protected amino acid precursors to prevent self-polymerization and enhance reactant vapor pressure, and a weak acid deprotectant ( $\text{H}_3\text{PO}_4$ ) to enable layer-by-layer ALD-type deposition of polypeptide films. We refined our process and confirmed the formation of uniform ca. 18 nm poly(L-alanine) films on the surface of silica nanoparticles (**Figure 19**), with ATR-FTIR and mass spectroscopies confirming the formation of a true poly(peptide) layer. Compared to conventional liquid-phase synthesis of polypeptides, ALD is faster and less labor-intensive, and has the potential to deposit materials with an arbitrary sequence of different precursors to produce custom-designed biometric structures.

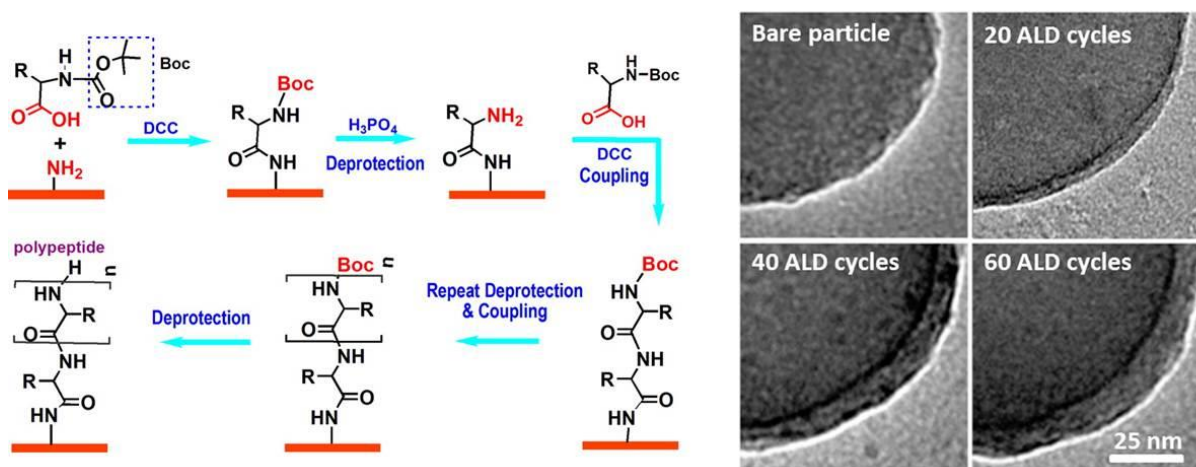


**Figure 19.** Schematic of the ALD reaction developed for the deposition of poly(L-alanine), along with TEM images of  $\text{SiO}_2$  particles with increasing number of ALD cycles. Fu et al., *J. Amer. Chem. Soc.*, October 30 2014.

### 3.5 Understand creation of biotic/abiotic interfaces and organisms

**Finding 1:** Used different tools of electron microscopy to discover a generalized mechanism whereby rare earth (RE) oxides serve to universally dephosphorylate bacterial organisms.

**Specifics:** Rare earth modification (REM) was used to study the creation of biotic and ‘abiotic’ behaviors (e.g. optical, catalytic, or magnetic properties) in bacterial cells.

Through REM, we discovered a generalized mechanism whereby rare earth oxides universally dephosphorylate both Gram-negative and Gram-positive bacterial cell walls and create a new rare earth phosphate (REPO<sub>4</sub>) modified phenotype according to the hypothesis that; trivalent REE ions supplied by dissolution of highly soluble RE oxides, hydroxides, carbonates, etc. are able to sequester any bioavailable phosphorous through the formation of highly insoluble RE phosphates dictated by:  $RE^{3+} + PO_4^{3-} \rightleftharpoons REPO_4$ , where pK<sub>sp</sub> ranges from 24.8 for Yttrium to 26.2 for Lanthanum and Ytterbium. REM occurs principally by binding to the phosphate based macromolecules expressed on the of Gram-negative and Gram-positive bacteria accompanied by the formation of needle or urchin-like REPO<sub>4</sub> crystals as demonstrated for Gram-negative (*E. coli* K12 T7 and *Salmonella typhimurium* LT2) and Gram-positive (*Staphylococcus aureus*) bacteria suspended in phosphate-free medium (**Figure 20**).

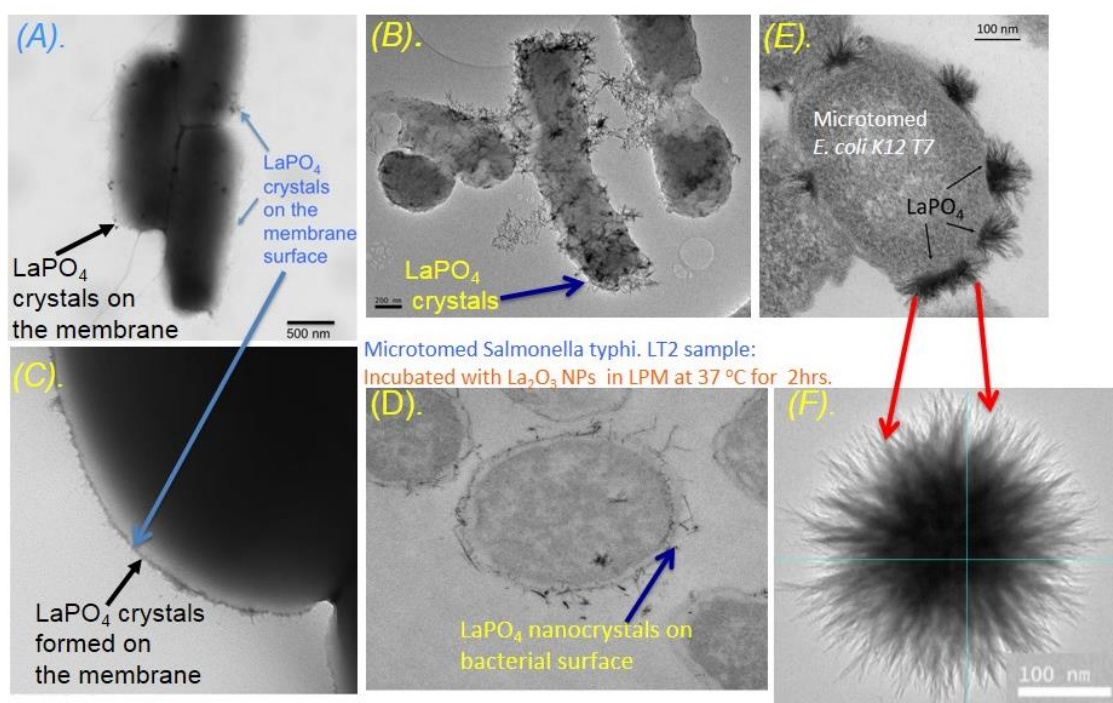


**Figure 20.** **A)** TEM image of *E. coli* K12 T7; **B)** *Salmonella typhimurium* LT2; **C)** *Staphylococcus aureus* after 2hr incubation with La<sub>2</sub>O<sub>3</sub> nanoparticles (NPs); **D).** Cross-sectional TEM analysis of microtomed *Salmonella typhimurium* LT2 after 120-minute incubation with La<sub>2</sub>O<sub>3</sub> NPs in limited phosphate medium; **E).** TEM image of *E. coli* K12 T7 incubated with 100 μg/ml CTAB templated LaCl<sub>3</sub> doped silica oxide NPS for 2hr, and **F)** LaPO<sub>4</sub> 'urchin' formed in simulated phagosomal fluid.

To help elucidate the process by which LaPO<sub>4</sub> crystals are formed on the bacterial membrane, we secured a time at the Center for Integrated Nanotechnologies (CINT) at Sandia National Laboratories, and used liquid cell *in situ* STEM instrument equipped with Hummingbird liquid TEM holder (5 nm nitride windows for the liquid cell, 300 kV accelerating voltage) to show that, initiation of LaPO<sub>4</sub> crystal growth is induced by cellular

stress beyond the presence of La (**Figure 21**).

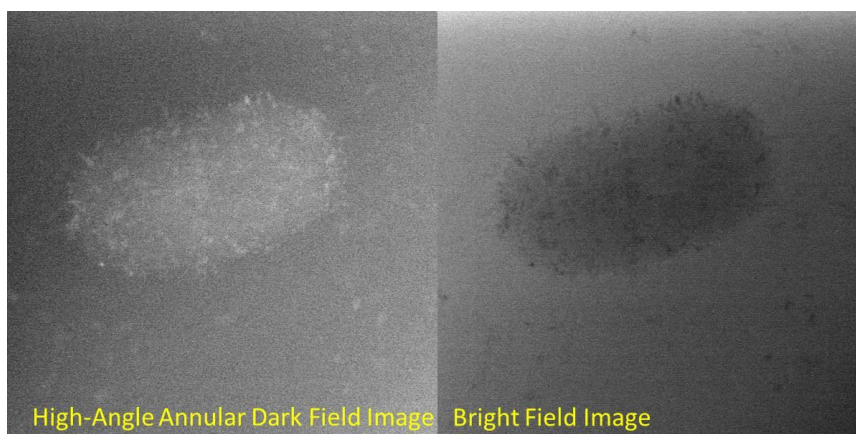


**Figure 21.** In situ liquid cell STEM imaging of living *E. coli* K12 T7 incubated with commercial La oxide NPs, showing growth of LaPO<sub>4</sub> crystals at the cell surface.

The results obtained by electron microscopy imaging prompted us to question if the RE modification of bacterial membrane is driven by the kinetics of the interactions of the RE and bacteria. Using model *Salmonella typhimurium* LT2, we confirmed the rapid (~ 15 minute) heterogeneous deposition of insoluble RE phosphate crystals on the surface of *Salmonella typhimurium* LT2 membrane (**Figure 22A,B**), followed by (after ~60 minutes), removal of RE phosphate nanostructures by physical sloughing, leaving only very small crystallites on the bacterial surface. In addition to diffraction data (**Figure 22C**), elemental mapping by EDS/SEM (**Figure 22D**), was consistent with the presence of REPO<sub>4</sub> at nanocrystal stoichiometry of 1 RE: 1 Phosphate. After 60 minutes, although the whisker and urchin nanostructures were largely gone, EDS showed a homogeneous distribution of RE across the surface of bacterial cell, including the presence of minute nanocrystals of RE phosphates (**Figure 22E**). This is suggested that REM is most likely driven by mass transfer of RE<sup>3+</sup> ions to the bacterial membrane.

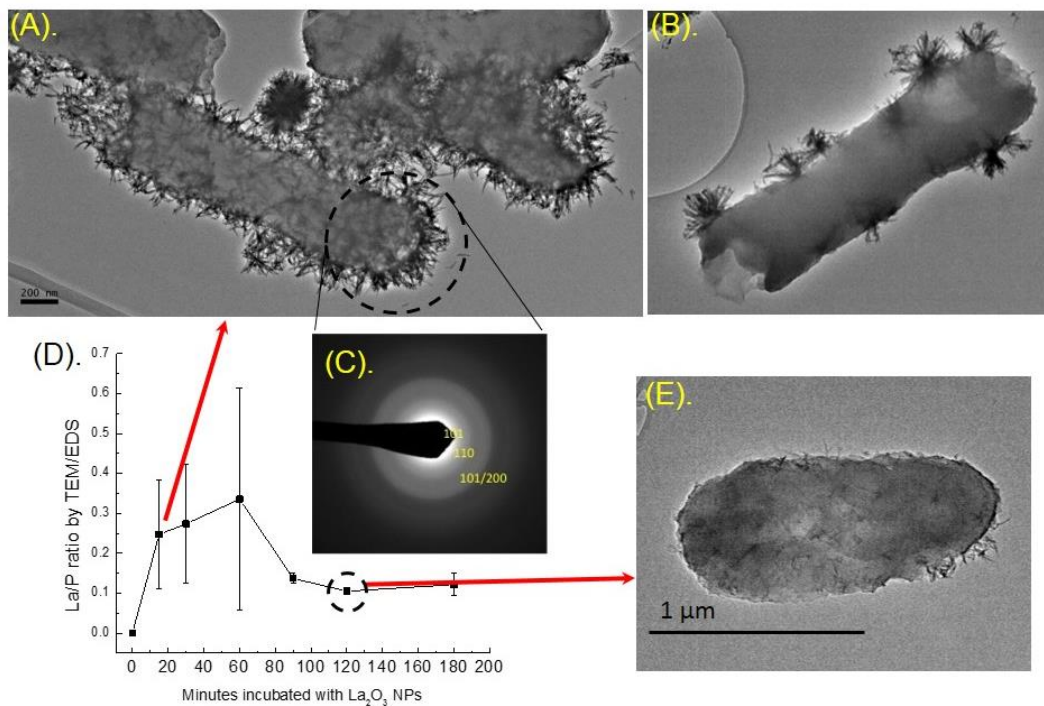


**Figure 22.** A). Rapid distribution of LaPO<sub>4</sub> crystals on the membrane of *Salmonella typhimurium* LT2 after 15-minute incubation in HEPES buffered limited phosphate medium (LPM) containing 100 μg/ml La<sub>2</sub>O<sub>3</sub> NPs, B). Distribution of 'urchin-like' LaPO<sub>4</sub> crystals on the membrane of *Salmonella typhimurium* LT2 after 15-minute incubation in HEPES buffered limited phosphate medium containing 100 μg/ml La<sub>2</sub>O<sub>3</sub> NPs, C). Selected area diffraction (SAD) analysis of LaPO<sub>4</sub> crystal-modified *Salmonella typhimurium* LT2 after 15-minute incubation. Phosphate whiskers were confirmed to be crystalline with significant amount of disorder, D). Deduced La/P ratio for *Salmonella typhimurium* LT2 modified with LaPO<sub>4</sub> crystals and E). Representative TEM image of *Salmonella typhimurium* LT2 at 180-minute incubation with 100 μg/ml La<sub>2</sub>O<sub>3</sub> NPs. Reduced whiskers at longer times suggestive of ejection of crystalline features

**Finding 2:** Used electron microscopy combined with luminescence measurements to demonstrate formation of binary rare earth phosphates on the bacterial membrane.

**Specifics:** In order to elucidate if there is species selectivity for binary RE stoichiometry on the bacterial membrane, we investigated the formation of binary RE phosphates on the surface of bacteria. Fundamentally, such binary materials can be versatile means of adding optical or catalytic functionalities to bacterial organisms. Using a binary mixture of oxides of lanthanum and europium (optically active RE), we confirmed that, *Salmonella typhimurium* LT2 incubated with mixture of lanthanum and europium oxides resulted in

binary ‘doped’ rare earth phosphate nanocrystals on the bacterial surface (**Figure 23**), and the interaction also conferred binary RE stoichiometry and luminescence characteristics on the bacterial membrane (**Figure 23**). The overall atomic ratios of these two elements in the binary phosphate mixture were found to be similar to that of pure phosphate nanoparticles (**Figure 23**), indicating that no enrichment of one RE over the other occurred. However, fluorescence data demonstrated that the chemical environment of Eu as a function of Eu/La was dissimilar for phosphates grown on bacterial membranes in comparison to free phosphate nanoparticles.

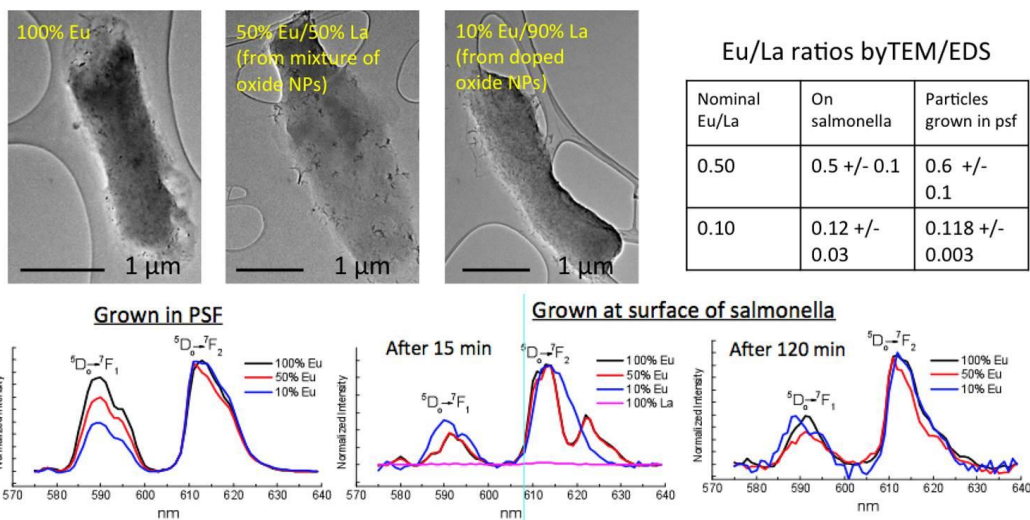


**Figure 23.** Top: TEM images of *Salmonella typhi*. LT2 incubated with binary mixture of  $\text{Eu}_2\text{O}_3$  and  $\text{La}_2\text{O}_3$  NPs as RE sources, along with elemental ratios of Eu/La determined by EDS for modified bacteria and phosphate particles grown in phagosomal simulated fluid (PSF). Bottom: Luminescence spectra of  $\text{EuPO}_4$  nanocrystals formed/grown in PSF compared with the nanocrystals formed on the surface of *Salmonella typhi*. LT2, showing narrowing of the spectra with time due to ejection of bulk RE phosphate crystals.

**Finding 3:** Used different tools including biochemical assays, wide field and confocal microscopy to demonstrate the effect of rare earth modification (REM) on bacterial growth, physiological changes, motility, behavior, and interactions with ‘professional’ phagocytic cells.

**Specifics:** Evidence of rare earth modification prompted us to also question if this phenomenon could impact various aspects of bacterial organisms including bacterial growth, physiological changes (induced oxidative stress, altered enzymatic activity, induced metabolic changes), motility and behavior, and interactions of  $\text{REPO}_4$  modified bacteria with ‘professional’ phagocytic cells. On growth, we assessed REM effect on the growth of Gram-negative (*Salmonella typhimurium* LT2) and Gram-positive (*Staphylococcus aureus*) bacteria suspended in both standard medium (LB/TSB) and limited phosphate medium (LPM) supplemented with a fixed concentration of REO. REO was not inhibitory to bacterial growth in standard (LB or TSB) medium (**Figure 24 A,C**),

but exhibited differential inhibition of bacterial growth in limited phosphate medium (LPM) [Figure 24 B,D], suggestive of toxicity caused by phosphate starvation due to binding of free  $\text{PO}_4^{3-}$  ions with RE ions in solution. Lack of growth inhibition in standard nutrient rich LB/TSB medium was attributed to optimal phosphate levels. On the impact of RE modification on metabolic indicators, we assessed the levels of intracellular ATP and lipid droplets levels as respective metabolic indicators of respiratory rate changes and induced starvation responses in  $\text{LaPO}_4$  modified *Salmonella typhi*. LT2. Lanthanum nanoparticle ( $\text{La}_2\text{O}_3$ ) concentration dependent increase of intracellular ATP levels was noted (Figure 25A), suggestive of combined effects of altered metabolic rate due to lanthanum depletion of phosphates and possible inside out loss of phosphate molecules to the extracellular surface. Higher intracellular ATP level was consistent with induced buildup of cytoplasmic lipid droplets (Figure 25B), as evidence of dephosphorylation dependent starvation.

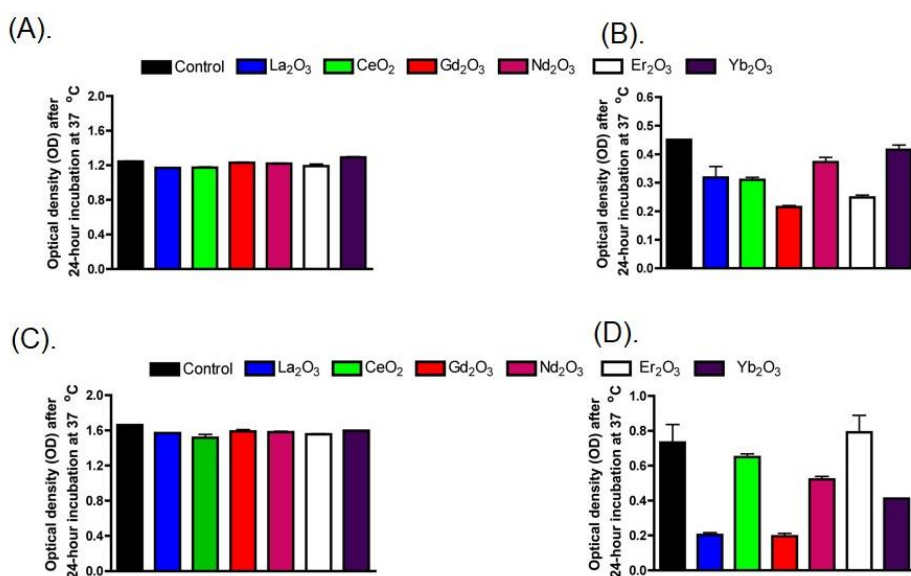


**Figure 24.** **A).** Optical density of *Salmonella typhimurium* LT2 after 24hr incubation with  $\text{La}_2\text{O}_3$  NPs in standard LB medium; **B).** Optical density of *Salmonella typhimurium* LT2 after 24hr incubation with  $\text{La}_2\text{O}_3$  NPs in limited phosphate medium (LPM); **C).** Optical density of *Staphylococcus aureus* after 24hr incubation with  $\text{La}_2\text{O}_3$  NPs in standard LB medium and, **D).** Optical density of *Staphylococcus aureus* after 24hr incubation with  $\text{La}_2\text{O}_3$  NPs in limited phosphate medium. Where applicable, bacterial samples were incubated with 100  $\mu\text{g}/\text{ml}$   $\text{La}_2\text{O}_3$  NPs before OD measurements.

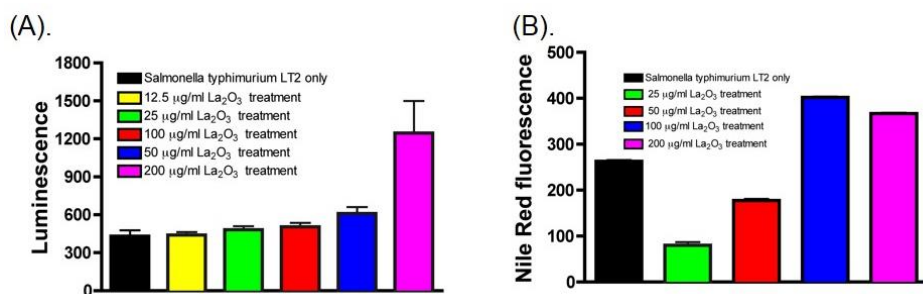


**Figure 25.** A). Intracellular ATP levels in *Salmonella typhimurium* LT2 after 2hr incubation with La<sub>2</sub>O<sub>3</sub> NPs and B). Lipid droplet levels in *Salmonella typhimurium* LT2 after 2hr incubation with La<sub>2</sub>O<sub>3</sub> NPs. Samples were incubated with nanoparticles in limited phosphate medium.

Reactive oxygen species such as superoxide anion radical (O<sup>-</sup>), hydrogen peroxide (H<sub>2</sub>O<sub>2</sub>), highly reactive hydroxyl radicals (<sup>•</sup>OH) and other peroxides always accompany aerobic growth of bacterial organisms as byproducts of metabolic processes. CM-H<sub>2</sub>DCFDA probe, which relies on the cleavage of DCFH-DA by intracellular esterases to produce the relatively polar and cell membrane-impermeable fluorescent product, H<sub>2</sub>DCF was used to assess levels of total reactive oxygen species (ROS) in LaPO<sub>4</sub> modified *Salmonella typhimurium* LT2. We noted time and La<sub>2</sub>O<sub>3</sub> concentration dependent ROS release (Figure 26 A), concordant with the La<sub>2</sub>O<sub>3</sub> concentration dependent increase in the levels of alkaline phosphatase (AP) enzyme (Figure 26B). Higher levels of AP confirmed dephosphorylation based enhanced phosphate transfer mechanisms and possible corresponding increased synthesis of phosphomonoester substrate compounds. Together, these physiological changes confirmed that REM potentially impacted various intracellular pathways in LaPO<sub>4</sub> modified *Salmonella typhimurium* LT2.

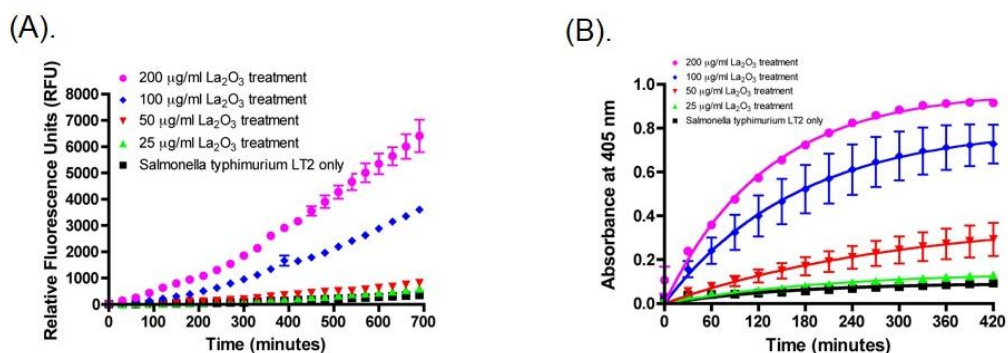


**Figure 26.** A). Global reactive oxygen species (ROS) release by LaPO<sub>4</sub> modified *Salmonella typhimurium* LT2 and B). Alkaline phosphatase (AP) activity in LaPO<sub>4</sub> modified *Salmonella typhimurium* LT2. para-Nitrophenyl phosphate (pNPP) substrate was used to test the activity of alkaline phosphatase enzyme derived from the clarified bacterial lysate. Where applicable, samples were incubated with La<sub>2</sub>O<sub>3</sub> NPs for 2hr before respective measurements.

Bacterial behavior and related motility encompass biofilm formation, swimming (single cell movement) and swarming (multicellular movement). By definition, bacterial biofilms are characterized by complex cell assemblages buried in an adherent matrix structure, exhibiting channels and pillars to facilitate nutrient exchange and elimination of metabolic waste. Exo-polymer materials like lipopolysaccharide (LPS) are critical to the bacterial biofilm formation (**Figure 27A**). We characterized the effect of REM on the biofilm formation by *Salmonella typhimurium* LT2 incubated with  $\text{La}_2\text{O}_3$  NPs. Biofilms with distinct morphological differences were confirmed in the presence of  $\text{La}_2\text{O}_3$  nanoparticles. While the control (*unexposed to lanthanum*) formed isolated rdar morphotype (multicellular behavior) biofilms (**Figure 27B**), the  $\text{LaPO}_4$  modified *Salmonella typhimurium* LT2 formed biofilms dominated by individual bacterial cells (**Figure 27B**). Biofilms formed by  $\text{LaPO}_4$  modified *Salmonella typhimurium* LT2 suggested dephosphorylation driven enhanced synergistic synthesis of exo-polymer materials (including LPS) necessary for biofilm formation. Significantly, accelerated lanthanum driven biofilm formation can potentially generate useful bio-corrosion inhibitor platforms for metal surfaces.

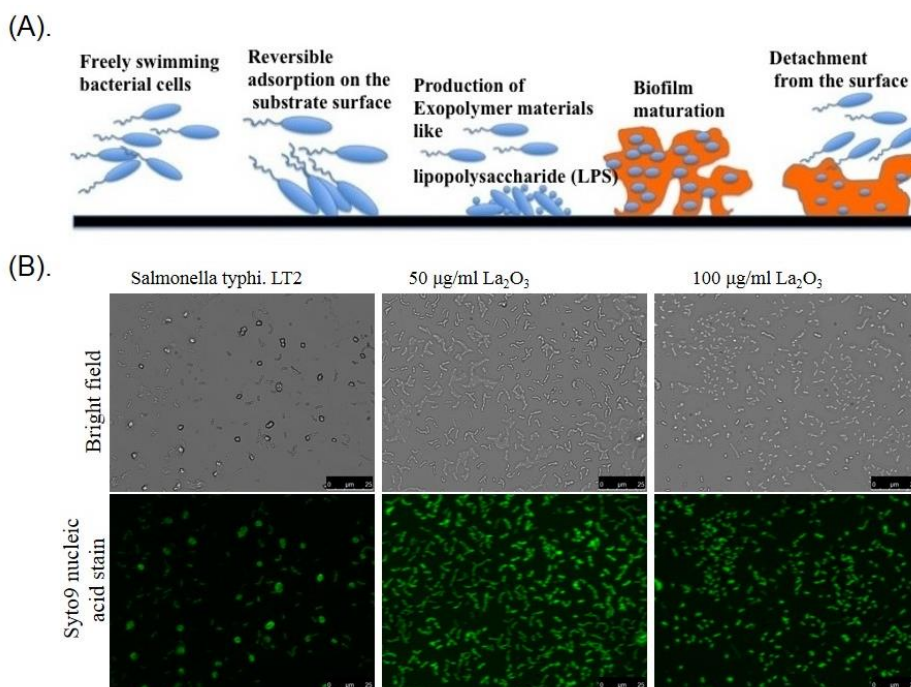


**Figure 27. A).** Evolution of biofilm formation by Gram-negative bacterial cells. Reversible adsorption of individual bacterial cells is followed by irreversible adsorption phase which is aided by cell to cell communication via quorum sensing. Biofilm maturation is characterized by cell division and recruitment. **B).** Biofilm formation by  $\text{LaPO}_4$  modified *Salmonella typhimurium* LT2 incubated for 48hr in standard LB medium containing  $\text{La}_2\text{O}_3$  NPs. Lanthanum depletion of bacterial  $\text{PO}_4^{3-}$  ions potentially triggers synthesis of more LPS molecules that contribute to enhanced biofilm attachment to the surface.

Typically, bacterial biofilm formation runs in tandem with bacterial motility. Consistent with the enhanced biofilm formation by LaPO<sub>4</sub> modified *Salmonella typhimurium* LT2, we confirmed that REM alters bacterial motility by inducing a time-dependent delay in swimming motion/motility of *E. coli* K12 T7 (**Figure 28A**), and also, triggering the generation of dendrite-like swarming patterns by LaPO<sub>4</sub> modified *Salmonella typhimurium* LT2 (**Figure 28B**). These findings were suggestive of enhanced synthesis and release of macromolecules like LPS necessary for the collective behavior of these bacteria. Relatedly, physical blockage of LPS and may be other phosphate based pathogen-associated molecular patterns, PAMPs within the outer membrane, was confirmed by the obscuration of *Salmonella typhimurium* LT2 by LaPO<sub>4</sub> which prevented recognition and uptake of LaPO<sub>4</sub> modified *Salmonella typhimurium* LT2 by mammalian mouse macrophage Raw264.7 cells (**Figure 29**).

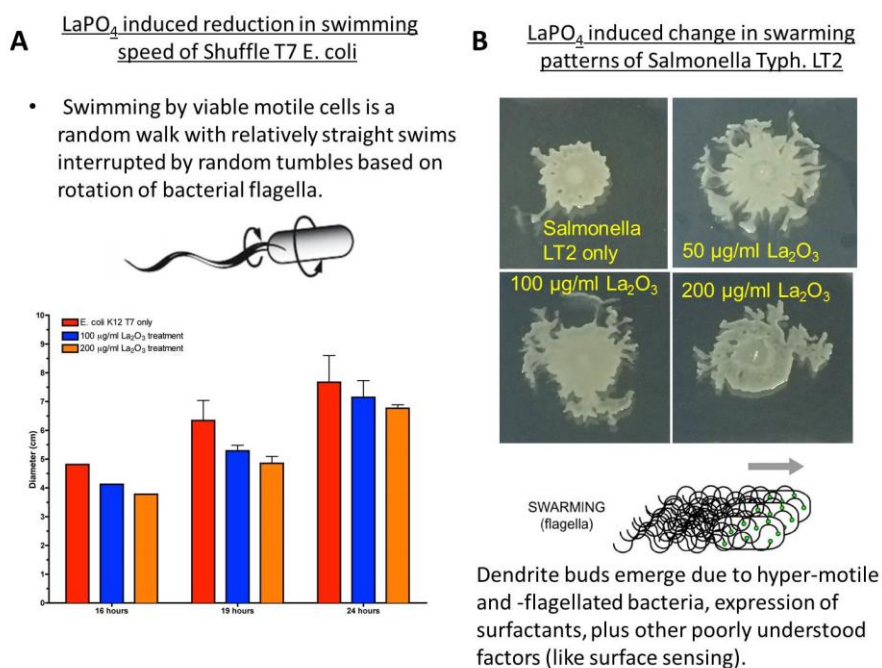


**Figure 28.** A). Time and concentration dependent reduction in swimming motility of *E. coli* K2 T7 modified with LaPO<sub>4</sub> nanocrystals, and B) LaPO<sub>4</sub> mediated evolution of dendrite-like swarming patterns of *Salmonella typhimurium* LT2.

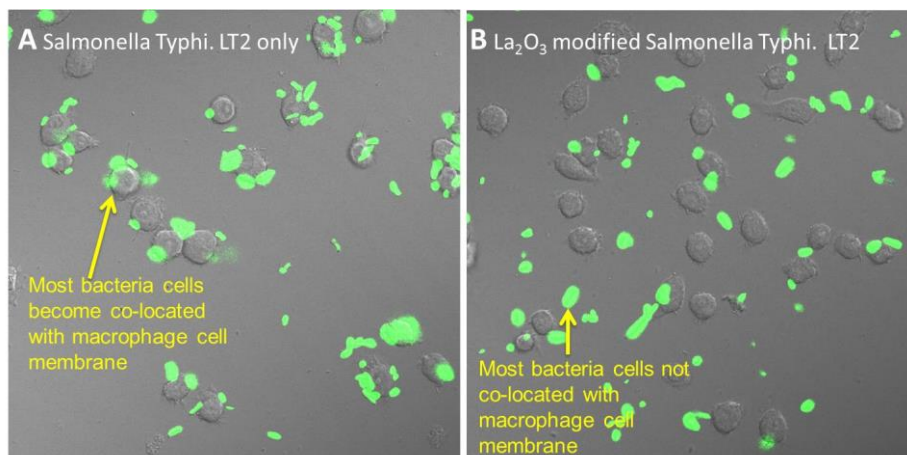


**Figure 29. A).** Control green fluorescent protein (GFP) expressing *Salmonella typhi. LT2* interacting with adherent mouse macrophage Raw264.7 cells, and **B).** LaPO<sub>4</sub> modified GFP-*Salmonella typhi. LT2* interacting with adherent mouse macrophage Raw264.7 cells. The interaction is based on the recognition of lipopolysaccharide (LPS) and other PAMPs by cell surface receptors of the Raw264.7 cells.

**Finding 4:** Used mathematical tools (Rietveld refinement and Fourier analysis), and liquid chromatography-mass spectrometry to perform structural analysis of LaPO<sub>4</sub> formed on the bacterial surface and elucidate mechanism of dephosphorylation respectively.

**Specifics:** In order to explain the sources of phosphorous that combine with RE ions to form REPO<sub>4</sub> crystals on the bacterial membrane, we carried out molecular mass analysis of LaPO<sub>4</sub> modified bacteria. Through our collaborators at University of California Center for Environmental Implications of Nanotechnology (UC CEIN), we used liquid chromatography-mass spectrometry analyses to confirm that RE modification leads to the dephosphorylation of phosphatidic acid (PA) on the membrane of *Salmonella typhi. LT2* (**Figure 30**). This was confirmed by the presence of dephosphorylated forms of PA in the sample derived from LaPO<sub>4</sub> modified *Salmonella typhi. LT2*. This is a significant finding because phosphatidic acid is a biosynthetic precursor for the formation of all acylglycerol lipids in the bacterial cell.

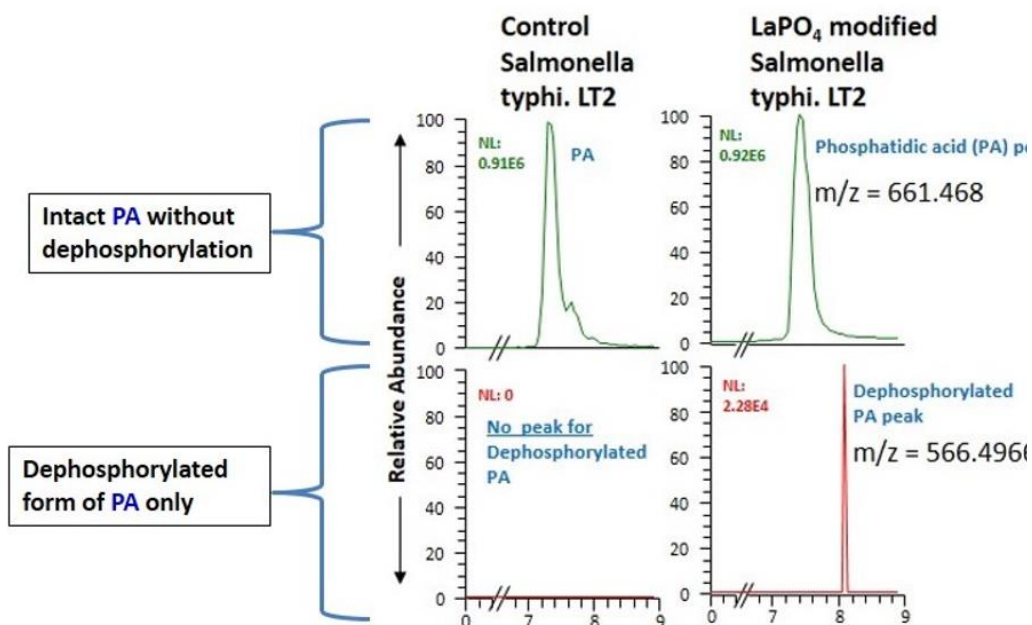


**Figure 30.** Liquid chromatography-mass spectrum of LaPO<sub>4</sub> modified *Salmonella typhimurium* LT2 showing evidence of dephosphorylated membrane phosphatidic acid (PA). *Salmonella typhimurium* LT2 was incubated with La<sub>2</sub>O<sub>3</sub> NPs (100 µg/ml) in limited phosphate medium and then subjected to analyses after appropriate

As a way of understanding the nature of REPO<sub>4</sub> formed on the bacteria membrane, we refined the structure of the trigonal REPO<sub>4</sub> formed by early group of RE elements (**Figure 31**). Although many nanoparticle syntheses of REPO<sub>4</sub> have been reported with this crystal structure, an atomic level understanding of several important material properties (e.g. instability to heating, inaccessibility of micropores, or preferred 1D growth of nanomaterials) has been lacking. Using a combination of Rietveld refinement and Fourier analysis of LaPO<sub>4</sub> crystal grown under conditions where crystallite size is maximized, we found evidence of water molecule present within the micropore channels of this material. This water molecule blocks access into the channels, and satisfies the requirement for 9-fold coordination around La centers. Sample heating drives off this water molecule via evaporation, and induces a phase change to reestablish the preferred environment around La atom. Also, 1D growth of La (and other early group REs) appears to be driven by strong bidentate binding of phosphate to La along the c-axis of the crystal structure.

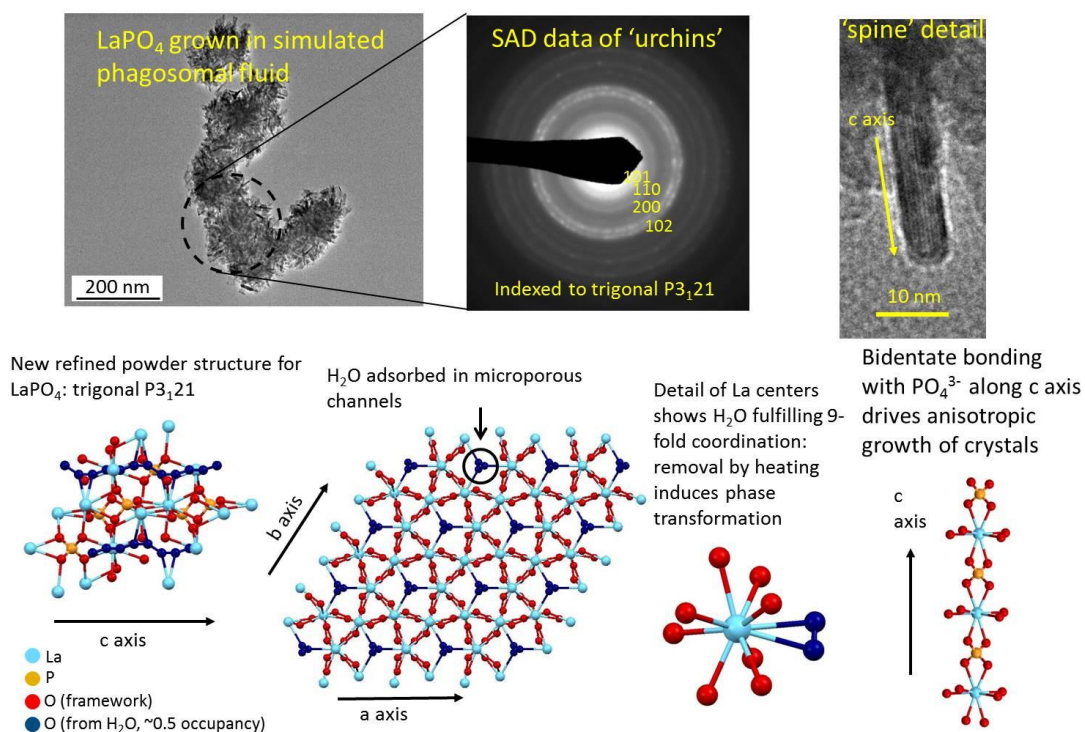


**Figure 31.** Structural analysis of LaPO<sub>4</sub> as formed on the surface of bacteria in the presence of RE oxide nanoparticles.

Taken together, REEs occur at different levels in nature dictated by the unique geological characteristics of the environmental settings. For instance, lanthanum which represents a good candidate for the study of RE-microbial interactions, constitutes up to 18 ppm of the earth's crust. Currently, little is known about the interactions of REEs with bacterial organisms despite increasing use of these elements in many applications. Rare earth phosphate modified bacteria therefore represent a newly discovered class of living biotic/abiotic phenotypes that could potentially possess a unique combination of properties including insolubility, thermal stability, low toxicity, catalytic activity, and high quantum yield such that 'doping' with other rare-earth ions (LaPO<sub>4</sub>: Ln<sup>3+</sup>; Ln = Ce, Sm, Gd, Tb, Sr, etc) could lead to the formation of highly photo-stable bioprobes with novel and potentially species-specific luminescence. Moreover, RE modification of bacteria suggests further investigations of bacterial organisms derived from RE-rich environments as possible biomining agents for RE enrichment/concentration purposes.

**Finding 5:** Used chemical synthesis methods to prepare metal organic framework (MOF) compound and cell culture techniques to understand how MOF impacts mammalian cell viability and tolerance of extreme conditions.

**Specifics:** Metal-organic frameworks (MOFs) are gaining interests of many investigators due to their increasing applications in gas storage devices, purification and separation materials, catalysts and sensors. They are crystalline materials consisting of coordination bonds between transition-metal cations (e.g.  $Zn^{2+}$ ) and multidentate organic linkers and are characterized by open frameworks that can be porous enough to delay transport of small molecules (**Figure 32**). We investigated the ability of MOF (ZIF-8-TA shell) coating to functionalize live mammalian cells based on their complex chemical structure. We established that MOF modification of HeLa cells created a conformal cell wall that can impart mechanical strength as well as endow mammalian cells with new properties and behaviors (**Figure 33B-D**). MOF coating was able to induce spore-like hibernation state to HeLa cells such that while the cells lost their abilities to adhere to the extracellular matrix (**Figure 33F**), they remained viable in this state as confirmed by the adhesion and replication of MOF coated HeLa cells upon removal/etching of the MOF layer with ethylenediaminetetraacetic acid (EDTA) solution (**Figure 33 G-I**).

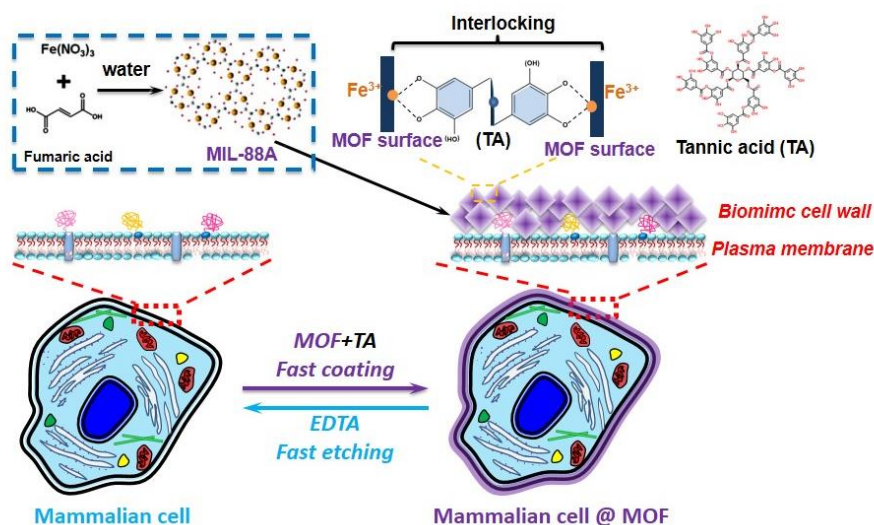
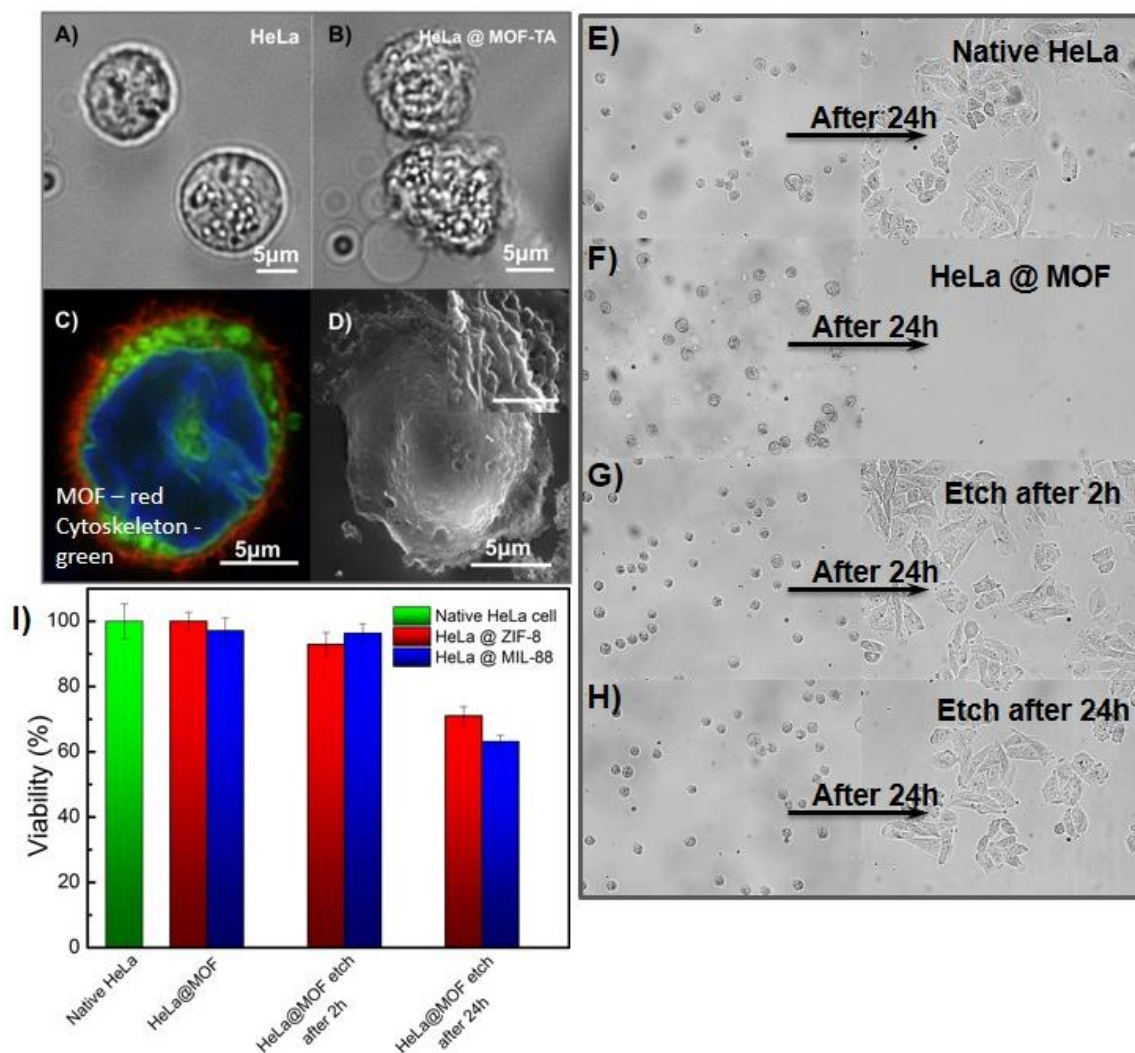


**Figure 32.** Depiction of the design and chemistry of the metal organic framework (MOF) coating of mammalian cell wall. MOFs are bound to cell membrane via coordination of metal centers with adsorbed polyphenols (e.g. TA). This ‘new’ cell wall can endow mammalian cells with new properties and behaviors such as tolerance to extreme conditions.



Significantly, we also confirmed that MOF coated HeLa cells displayed better extremophile-like characteristics than the native cells (**Figure 34A-D**). This was exemplified by their better tolerance of high salt strength (**Figure 34B**) and UV exposure (**Figure 34D**) than the native HeLa cells. Better tolerance of low and high salt strength was aided by MOF's ability to adsorb large amounts of ions into their porous structure and delay ion transfer from solution to cell or cell to solution, thereby ensuring cell viability under low and high salt concentrations (**Figure 34A**). More so, MOFs have high UV absorbance around 260nm (UVC) and 300nm (UVB) [**Figure 34C**] and this property can endow MOF coated cells with better UV tolerance characteristics. This can provide a basis to load MOFs with dyes that can absorb UVA to protect cells from UVA damage in the event of an exposure.

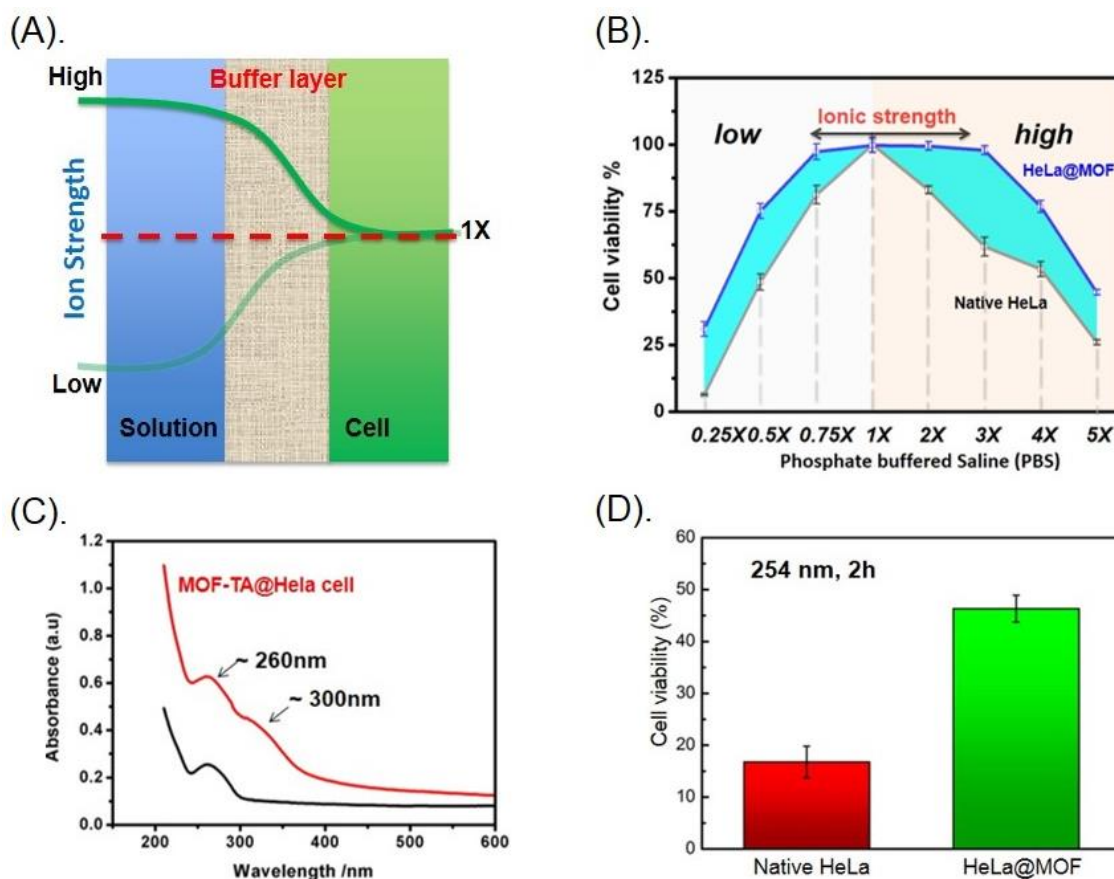


**Figure 34.** **A)** Depiction of salt strength buffer layer; **B)** Tolerance of MOF (ZIF-8-TA) coated HeLa cells to low and high salt strengths; **C)** UV-Vis spectrum of MOF (ZIF-8-TA) coated HeLa cells, and **D)** Tolerance and viability of MOF (ZIF-8-TA) coated HeLa cells to UV exposure.

## 4.0 Supporting Information for 1 February 2014 to 31 January 2017

### 4.1 Supported Personnel

- **Faculty:** C. Jeffrey Brinker
- **Research Staff:** Jason Townson PhD, Research Assistant Professor, Center for Micro-Engineered Materials, UNM, (*to Oncothyreon*); Ying-Bing Jiang PhD, Research Assistant Professor, Earth & Planetary Sciences, Manager, TEM/FIB Laboratory; Darren Dunphy, Research Associate Professor, UNM (*to Lumileds*); Jacob Agola, Research Assistant Professor, UNM, and Rita Serda, Research Assistant Professor, UNM.
- **Graduate Students** (est graduation date where applicable)
  - Paul Durfee, Biomedical Engineering, PhD 2016
  - Sherif Aboubakr, MS Nanoscience & Microsystems
  - Jimin Guo, PhD Chemical Engineering, est May 2019
  - Terisse Brocato, PhD Chemical Engineering, est May 2017
  - Patrick Johnson, PhD Nanoscience & Microsystems, est June 2017
- **Undergraduate students** (est graduation date where applicable)
  - Cameron Burgard, Biochemistry, BS 2015
  - Lauren Bustamante, Mechanical Engineering, BS 2015, (to MIT)
  - Richard Abraham, Mechanical Engineering, BS 2015 (to Stanford)
  - Amanda Lokke, Biochemistry, BS 2016
  - Ayse Muniz, Biochemistry, BS 2016, (to UMich)
  - Michael Salazar, Chem/Biol Engr, BS 2016, (to UCSD)
  - Yasmine Awad, Biochemistry/College of Pharmacy, est May 2017
  - Keoni Baty, Chemistry, BS est May 2018
  - Edward Wyckoff, Chem Eng. BS est May 2018
- **Post-docs**
  - Christophe Theron PhD, Ecole Nationale Supérieure de Chimie de Montpellier, France
  - Stan Chou PhD, Northwestern University, to Sandia National Labs
  - Achraf Nourenddine PhD, Ecole Nationale Supérieure de Chimie de Montpellier, France
  - Wei Zhu PhD, Peking University
  - Yaqin Fu PhD, University of New Mexico, Center for Micro-Engineered Materials.

#### 4.2 Collaborators -- groups outside of your lab who are participating in your basic research project

- Jacob O. Agola, Center for Micro-Engineered Materials, University of New Mexico- rare earth interactions with bacteria and ecosystems
- David Peabody, UNM Molecular Genetics and Microbiology, VLP phage display and VLP-directed materials deposition
- Graham Timmins, UNM Pharmacology - dormancy of TB, Quorum Sensing, and cell immobilization in silica matrices
- Hattie Gresham, UNM Molecular Genetics and Microbiology - Quorum Sensing
- Bryan Kaehr, SNL and UNM, multiphoton lithography of proteins scaffolds and architectures
- Kimberly Butler PhD, Bioenergy and Defense Technologies Department, Sandia National Laboratories, Albuquerque, NM 87185 - Nanobiology related research
- Rita Serda, PhD, Center for Micro-Engineered Materials, University of New Mexico- Advanced imaging and silica cell replication research.
- Rajesh Naik, US Air Force Research Laboratory, Au binding peptides. Peptide directed material deposition
- Fran Nargi, MIT Lincoln Laboratory, Biosensor and Molecular Technologies, CANARY cell-based sensing line
- Sveltana Harbaugh, US Air Force Research Laboratory, riboswitch integration into 3D matrices created by CDA/CDI and sol-gel entrapment
- Nancy Kelley-Loughnane and Morley Stone, US Air Force Research Laboratory, Riboswitches – integration into orthogonal fluidic platform
- Carlee Ashley, Sandia National Laboratories, Bioengineering and Biotechnology Dept., Livermore, CA , immunofluorescence assays of biofunctionality
- Jie Sun, Zeeshan Fazal, and Eric Jakobssen, University of Illinois, Protocells as platforms for synthetic biology, bioinformatics studies of gene expression for immobilized cells
- Gavin Pickett, Jamie Padilla, Keck-UNM Genomics Resource, UNM Cancer Center/UNM Clinical Translational Science Center, flow cytometry
- David Kaplan, Tufts University, silicification of silk
- Atul Parikh, UC Davis, cell replica supported lipid bilayers
- Mahmoud Taha, UNM, Nanoindentation studies of silica cell replicas
- Jason Harper, Sandia National Labs, 3D encapsulation of enzymes and cell in silica matrices, cell-based sensing
- Ying-Bing Jiang and Yaqin Fu, UNM, ALD, enzyme immobilization in nanoporous membranes
- Fritz Vollrath, Oxford, silicification of spiders and spider silk

- Lucio Ciacchi, University of Bremen, molecular simulations of membrane silica interactions
- Pavan Muttli, UNM, spray-drying of cell silica composites.
- Nathan Mara and Bill Nook, Sandia/Los Alamos National Laboratories, Center for Integrated Nanostructures – nanoindentation studies of silica bio/nanocomposites
- Marjo Yliperttula Group, University of Helsinki, silica replication of Stem cells
- Susan Rempe and Juan Vanegas, Sandia Labs, molecular simulations of nanoconfined enzymes
- Andre Nel Group, UCLA, Trish Holden Group UCSB, rare earth interactions with bacteria and ecosystems
- Carlee Ashley, Sandia National Laboratories, Bioengineering and Biotechnology Dept., Livermore, CA, immunofluorescence assays of biofunctionality.

#### **4.3 Archival publications (published) during reporting period (acknowledge AFOSR support, full or partial):**

##### **4.3.1 Published manuscripts**

1. Fu, Y.; Li, B.; Jiang, Y.-B.; Dunphy, D.; Tsai, A.; Tam, S. Y.; Fan, H. Y.; Zhang, H.; Rogers, D. M.; Rempe, S. B.; Atanassov, P.; Cecchi, J. L.; Brinker, C. J.: Atomic Layer Deposition of L-Alanine Polypeptide. *Journal of the American Chemical Society* **2014**, *136*, 15821-15825.
2. Chou, S. S.; Huang, Y.-K.; Kim, J.; Kaehr, B.; Foley, B. M.; Lu, P.; Dykstra, C.; Hopkins, P. E.; Brinker, C. J.; Huang, J.; Dravid, V. P.: Controlling the metal to semiconductor transition of MoS<sub>2</sub> and WS<sub>2</sub> in solution. *JACS* **2015**, *137*, 1742-1745.
3. Townson, J. L.; Lin, Y.-S.; Chou, S. S.; Awad, Y. H.; Coker, E. N.; Brinker, C. J.; Kaehr, B.: Synthetic fossilization of soft biological tissues and their shape-preserving transformation into silica or electron-conductive replicas. *Nat Commun.* **2014 Dec** *8*;5:566
4. Zhu, J.; Quan, Z.; Lin, Y.-S.; Jiang, Y. B.; Wang, Z.; Zhang, J.; Jin, C.; Zhao, Y.; Liu, Z.; Brinker, C. J.; Zxu, H.: Porous Ice Phases with VI and Distorted VII Structures Constrained in Nanoporous Silica. *Nano Letters* **2014**, *14*, 6554-6558.
5. Li, R.; Ji, Z.; Chang, C. H.; Dunphy, D. R.; Cai, X.; Meng, H.; Zhang, H.; Sun, B.; Wang, X.; Dong, J.; Lin, S.; Wang, M.; Liao, Y.-P.; Brinker, C. J.; Nel, A.; Xia, T.: Surface Interactions with Compartmentalized Cellular Phosphates Explain Rare Earth Oxide Nanoparticle Hazard and Provide Opportunities for Safer Design. *ACS Nano* **2014**, *8*, 1771-1783.
6. Xiong, S.; Dunphy, D. R.; Wilkinson, D. C.; Jiang, Z.; Strzalka, J.; Wang, J.; Su, Y.; de Pablo, J. J.; Brinker, C. J.: Revealing the Interfacial Self-Assembly Pathway of Large-Scale, Highly-Ordered, Nanoparticle/Polymer Monolayer Arrays at an Air/Water Interface. *Nano Letters* **2013**, *13*, 1041-1046.
7. Townson, J. L.; Lin, Y.-S.; Agola, J. O.; Carnes, E. C.; Leong, H. S.; Lewis, J. D.; Haynes, C. L.; Brinker, C. J.: Re-examining the Size/Charge Paradigm: Differing in Vivo Characteristics of Size- and Charge-Matched Mesoporous Silica Nanoparticles. *Journal of the American Chemical Society* **2013**, *135*, 16030-16033.

8. Kendall, E. L.; Ngassam, V. N.; Gilmore, S. F.; Brinker, C. J.; Parikh, A. N.: Lithographically Defined Macroscale Modulation of Lateral Fluidity and Phase Separation Realized via Patterned Nanoporous Silica-Supported Phospholipid Bilayers. *Journal of the American Chemical Society* **2013**, *135*, 15718-15721.
9. Chou, S. S.; Kaehr, B.; Kim, J.; Foley, B. M.; De, M.; Hopkins, P. E.; Huang, J.; Brinker, C. J.; Dravid, V. P.: Chemically exfoliated MoS<sub>2</sub> as near-infrared photothermal agents. *Angew Chem Int Ed Engl* **2013**, *52*, 4160-4.
10. Brinker, C. J.; Clem, P. G.: Quartz on Silicon. *Science* **2013**, *340*, 818-819.
11. Sun, J.; Jakobsson, E.; Wang, X.; Brinker, C. J. Nanoporous silica-based protocells at multiple scales for designs of life and nanomedicine. *LIFE* **2015**, *5*(1): 214.
12. Sun, B.; Pokhrel, S.; Dunphy, D. R.; Zhang, H.; Ji, Z.; Wang, X.; Wang, M.; Liao, Y.-P.; Chang, C. H.; Dong, J.; Li, R.; Mädler, L.; Brinker, C. J.; Nel, A. E.; Xia, T. Reduction of Acute Inflammatory Effects of Fumed Silica Nanoparticles in the Lung by Adjusting Silanol Display through Calcination and Metal Doping. *ACS Nano* **2015**, *9*, 9357-9372.
13. Savage, T. J.; Dunphy, D. R.; Harbaugh, S. V.; Kelley-Loughnane, N.; Harper, J. C.; Brinker, C. J. Influence of Silica Matrix Composition and Functional Component Additives on the Bioactivity and Viability of Encapsulated Living Cells. *ACS Biomaterials Science & Engineering* **2015**, *1*(12): 1231-1238.
14. Nel, A. E.; Parak, W. J.; Chan, W. C. W.; Xia, T.; Hersam, M. C.; Brinker, C. J.; Zink, J. I.; Pinkerton, K. E.; Baer, D. R.; Weiss, P. S. Where Are We Heading in Nanotechnology Environmental Health and Safety and Materials Characterization? *ACS Nano* **2015**, *9*, 5627-5630.
15. Lou, Y.-R.; Kanninen, L.; Kaehr, B.; Townson, J. L.; Niklander, J.; Harjumäki, R.; Jeffrey Brinker, C.; Yliperttula, M. Silica bioreplication preserves three-dimensional spheroid structures of human pluripotent stem cells and HepG2 cells. *Scientific Reports* **2015**, *5*, 13635.
16. Johnson, P. E.; Muttill, P.; MacKenzie, D.; Carnes, E. C.; Pelowitz, J.; Mara, N. A.; Mook, W. M.; Jett, S. D.; Dunphy, D. R.; Timmins, G. S.; Brinker, C. J. Spray-Dried Multiscale Nano-biocomposites Containing Living Cells. *ACS Nano* **2015**, *9*, 6961-6977.
17. Harper, J. C.; Carson, B. D.; Bachand, G. D.; Arndt, W. D.; Finley, M. R.; Brinker, C. J.; Edwards, T. L. Laser Machined Plastic Laminates: Towards Portable Diagnostic Devices for Use in Low Resource Environments. *Electroanalysis* **2015**, *27* (11), 2503-2512
18. Dunphy, D. R.; Sheth, P. H.; Garcia, F. L.; Brinker, C. J. Enlarged Pore Size in Mesoporous Silica Films Templated by Pluronic F127: Use of Poloxamer Mixtures and Increased Template/SiO<sub>2</sub> Ratios in Materials Synthesized by Evaporation-Induced Self-Assembly. *Chemistry of Materials* **2015**, *27*, 75-84.
19. Dobroff, A. S.; Rangel, R.; Guzman-Rojas, L.; Salmeron, C. C.; Gelovani, J. G.; Sidman, R. L.; Bologna, C.; Opera, T.; Brinker, C. J. Ligand-directed profiling of organelles with internalizing phage libraries. *Current Protocol in Protein Science* **2015**, *30*, 1-30.34.
20. Chou, S. S.; Sai, N.; Lu, P.; Coker, E. N.; Liu, S.; Artyushkova, K.; Luk, T. S.; Kaehr, B.; Brinker, C. J. Understanding catalysis in a multiphasic two-dimensional transition metal dichalcogenide. *Nature Communications* **2015**, *6*.
21. Butler, K. S.; Durfee, P. N.; Theron, C.; Ashley, C. E.; Carnes, E. C.; Brinker, C. J., Protocells: Modular Mesoporous Silica Nanoparticle-Supported Lipid Bilayers for Drug Delivery. *Small* **2016**, *12* (16), 2173-85.

22. H. Hosoya, A.S. Dobroff, W.H. Driessen, V. Cristini, L.M. Brinker, F.I. Staquicini. Integrated nanotechnology platform for tumor-targeted multimodal imaging and therapeutic cargo release. *Proc Natl Acad Sci U S A*, 113 (2016), pp. 1877–1882.
23. B. Sun, X. Wang, Y.-P. Liao, Z. Ji, C.H. Chang, S. Pokhrel, J. Ku, X. Liu, M. Wang, D.R. Dunphy, R. Li, H. Meng, L. Mädler, C.J. Brinker, A.E. Nel, T. Xia. Repetitive dosing of fumed silica leads to pro-fibrogenic effects through unique structure-activity relationships and biopersistence in the lung. *ACS Nano*, 10 (2016), pp. 8054–8066.
24. MAG Porras, PN Durfee, AM Gregory, GC Sieck, CJ Brinker, CB Mantilla, A novel approach for targeted delivery to motoneurons using cholera toxin-B modified protocells. *Journal of Neuroscience Methods* Vol 273, 2016, 160–174.
25. P.N. Durfee, Y.S. Lin, D.R. Dunphy, A.J. Muniz, K.S. Butler, K.R. Humphrey, A.J. Lokke, J.O. Agola, S.S. Chou, I.M. Chen, W. Wharton, J.L. Townson, C.L. Willman, C.J. Brinker. Mesoporous silica nanoparticle-supported lipid bilayers (protocells) for active targeting and delivery to individual leukemia cells. *ACS Nano* (2016).
26. V.J. Yao, S. D'Angelo, K.S. Butler, C. Theron, T.L. Smith, S. Marchio, J.G. Gelovani, R.L. Sidman, A.S. Dobroff, C.J. Brinker, A.R. Bradbury, W. Arap, R. Pasqualini. Ligand-targeted theranostic nanomedicines against cancer. *J. Control. Release* (2016).

#### **4.3.2 Refereed Publications – *in preparation*:**

1. Dunphy, Darren; Bustamante, Lauren; Benavidez, Angelica; Datye, Abhaya; Dawson, Noel; Brinker, C. Jeffrey. Poloxamer-Templated 2D Nanopatterned Ultrathin Metal Oxide Films Synthesized with Evaporation-Induced Self-Assembly.
2. Jacob O. Agola, Darren Dunphy, Michael Salazar, Stephen Jett, Christophe Theron, Taylor McGregor, Alexander Prossnitz, Suman Pokhrel, Lutz Mädler, Paul Durfee, Patricia A. Holden, Ruibin Li, Andre Nel, and C. Jeffrey Brinker. Rare Earth Ions Universally Modify Bacterial Membranes Altering Bacterial Behavior and Mammalian Cell Recognition.
3. Zeeshan Fazal, Jennifer Pelowitz, Patrick E. Johnson, Jason C. Harper, C. Jeffrey Brinker, Eric Jakobsson. Creating distinct Metabolic States in Encapsulated Microbial Cells

#### **4.4 Other Publications/Presentations:**

##### **4.4.1 Books/Book Chapters:**

Brinker, C.J.: Dip-Coating. In *Chemical Solution Deposition of Functional Oxide Thin Films*; Schneller, T., Waser, R., Kosec, M., Payne, D., Eds.; Springer Vienna, 2013, pp 233-261.

**4.4.2 Invited Presentations:** presentations at international technical symposia, national labs, industry and universities: American Chemical Society (1), Materials Research Society (3), DOE (1), National Labs (3), Industry (2), Gordon Research Conferences (2), National Cancer Inst (1), Academia (4), Le Studium

Conference/Orlean, FR (1), International Conference on Multifunctional, Hybrid and Nanomaterials, Sorrento, Italy (1), DOE Basic Energy Sciences (1); Fourth International Conference on Multifunctional Hybrid and Nanomaterials, Sitges/Barcelona, Spain (Conference Organizing Committee, Session Chair, Featured Speaker); Third International Conference on Advanced Complex Inorganic Materials, Namur, Belgium; Biophysical Society Thematic Meeting: Polymers and Self-Assembly – From Biology to Nanomaterials, Rio de Janeiro, Brazil.

**4.4.3 Contributed Presentations:** presentations at international, national, regional technical symposia, national labs: American Chemical Society (1), Materials Research Society (15), National Cancer Inst (1), National Labs (3), Society for Advancement of Chicanos and Native Americans in Science - SACNAS (2)., Gordon Research Conference, Chemical-Biological Terrorism Defense (1); Chemical & Biological Defense and Technology Conference (2); Biomedical Engineering Society Annual meeting (2); American Society for Microbiology Annual meeting (1).

## 4.5 Awards / Honors / Service

### C. J. Brinker

- **2014** Federal Laboratory Consortium, Notable Technology Development Award, Nano-Stabilized Enzymatic Membrane for CO<sub>2</sub> Capture
- **2014** Elected to the Board of Directors, Materials Research Society
- **2014** Named to External Advisory Board of the NanoBio Node of the NSF-funded NanoHub - a resource for understanding and designing nanoBIO devices and systems - a collaboration between the University of Illinois at Urbana-Champaign and the University of California at Merced.
- **2015** UNM Science & Technology Center *Innovation Fellow Award*
- **2015** *R&D 100 Award, "Memzyme"*
- **2015** *R&D 100 Gold Medal in Green Technology*
- **2015** UNM *Presidential Medal of Distinction*.

### Students

- **Terisse Brocato** (PhD student) School of Engineering Award – the Charlotte and William Kraft Graduate Fellowship, the University of New Mexico, 2013-2015
- **Paul Durfee** (MS 2013, PhD student) **Best poster award** "Size and Surface Engineered Mesoporous Nanoparticles Direct Altered Biodistribution and Clearance", P. Durfee, Y.S. Lin, J. Townson, J. Minster, C.J. Brinker. Rio Grande Symposium on Advanced Materials, RGSAM, October 2014, Albuquerque, NM
- **Paul Durfee** (MS 2013, PhD student) George D. Montoya Research Scholarship, the University of New Mexico, 2013
- **Paul Durfee** (MS 2013, PhD student) **School** of Engineering Award – the Charlotte and William Kraft Graduate Fellowship, the University of New Mexico, 2013-2014.

- **Paul Durfee** (MS 2013, PhD student) **Edmund J. and Thelma W. Evans** Charitable Trust Scholarship, the University of New Mexico, 2013-2014.
- **Caroline Bouvie**, (MS student) **Best Presentation Award** “Mesoporous Oxide Nanoparticles for Controlled Release and Targeted Delivery of Antigens” Bouvie C.; Epler, K.; Padilla, D.; Gomez, A.; Anderson, M.; Fleig, P.; Chackerian, B.; Brinker, C. J.; Ashley, C. E.; Carnes, E. C. MRS Spring 2014 Meeting. Symposium Y: Biomaterials for Biomolecule Delivery and Understanding Cell-Niche Interactions. San Francisco, CA. April 2014. MRS Symposium Y.
- **Ayse Muniz** (Undergraduate student) STEM Public Policy Fellowship, the University of New Mexico, 2015
- **Ayse Muniz** (Undergraduate student) Maximizing Access to Research Careers Scholar, the University of New Mexico, 2014-2015
- **Ayse Muniz** (Undergraduate student) Arthur Friedman Scholarship, the University of New Mexico, 2014-2015
- **Ayse Muniz** (Undergraduate student) MIT Summer Research Program Scholar, Massachusetts Institute of Technology, 2015
- **Ayse Muniz** (Undergraduate student) SACNAS National Conference Travel Award, Society for Advancement of Chicanos/Hispanics and Native Americans in Science, 2015
- **Mina Aziz Faltas** (Undergraduate student) STEP internship, the University of New Mexico, 2015
- **Michael Salazar** (Undergraduate student) School of Engineering Award, Harry and Mabel F Leonard endowed scholarship, the University of New Mexico, 2013-2015
- **Terisse Brocato** (PhD student) The New Mexico Cancer Nanoscience and Microsystems Training Center (CNTC) Fellowship, the University of New Mexico, 2014-2015
- **Terisse Brocato** (PhD student) School of Engineering Award – the Charlotte and William Kraft Award, the University of New Mexico, 2014-2015
- **Paul Durfee** (MS 2013, PhD student) School of Engineering Award – the Charlotte and William Kraft Graduate Fellowship, the University of New Mexico, 2013-2015
- **Michael Salazar** (Undergraduate student) University of New Mexico NSF-STEM scholarship, the University of New Mexico, 2015
- **Terisse Brocato** (PhD student) School of Engineering Award – the Charlotte and William Kraft Graduate Fellowship, the University of New Mexico, 2015-2016.
- **Gabriel Garcia** (Undergraduate student) University of New Mexico Science, Technology, Engineering, and Mathematics Talent Expansion Program (STEP) Internship, 2016
- **Keoni Baty** (Undergraduate student) University of New Mexico STEP Internship, 2016
- **Keoni Baty** (Undergraduate student) National Science Foundation (NSF) STEP internship award, 2015-2016-

- **Keoni Baty** (Undergraduate student) National Science Foundation (NSF) STEP Travel Grant, 2015-2016
- **Keoni Baty** (Undergraduate student) Society of Women Engineers (SWE) Travel Grant, 2016
- **Keoni Baty** (Undergraduate student) National Science Foundation (NSF) STEP Mentor Award, 2016-Current
- **Keoni Baty** (Undergraduate student) New Mexico Lottery Scholarship, 2014-current
- **Antonella Riega** (Undergraduate student) University of New Mexico Nanoscience and Microsystems Research Experience for Undergraduates internship, 2016
- **Amanda Ramsdell** (Undergraduate student) University of New Mexico Nanoscience and Microsystems Research Experience for Undergraduates internship, summer 2015
- **Jacob Erstling** (Undergraduate student) University of New Mexico Nanoscience and Microsystems Research Experience for Undergraduates internship, summer 2015. STEP Internship, 2016.

#### **Postdocs and Research Faculty**

- **Jacob Ongudi Agola** (PhD 2011), Best Poster Award, Rio Grande Symposium on Advanced Materials, 3<sup>rd</sup> October, 2016, Albuquerque, NM.
- **Wei Zhu**, International postdoctoral exchange fellowship (China, 20140063) 04/01/15-04/01/17
- **Rita Serda** (PhD 2006), UNM Cancer Center Pilot Program Fellowship, Cancer Therapeutics, Selwyn, Serda, Brinker, Norenberg; 10/31/2016 – 11/11/2017.
- **Rita Serda** (PhD 2006), FEI Image Contest, Dual Beam, University of New Mexico, September 2016
- **Jacob Ongudi Agola** (PhD 2011), American Society for Microbiology (ASM) Travel Grant. New Orleans, LA., 2015.
- **Yu-Shen Lin** (U. Minnesota; post-doc) Center for Nanotechnology in Cancer Fellowship, the University of New Mexico, 2013-2014.

#### **4.6 Intellectual Property**

**Issued / allowed patents: February 1, 2014 – January 31, 2017** (partial AFOSR support)

<b>Patent #</b>	<b>Type</b>	<b>Issue/Filed Date</b>	<b>Country of Filing</b>	<b>Intellectual Property Title</b>
8,663,742	National	3/4/2014	United States	Durable Polymer/Aerogel Based Superhydrophobic Coatings, A Composite Material

8,734,816	National	5/27/2014	United States	Porous Nanoparticle Supported Lipid Bilayer Nanostructures
8,864,045	Utility	10/21/2014	United States	Aerosol Fabrication Methods for Monodisperse Nanoparticles
14/157,918	National	1/17/2014	United States	Durable Polymer/Aerogel Based Superhydrophobic Coatings, A Composite Material
13/869,799	Utility	4/23/2013	United States	Cell-based Composite Materials with Programmed Structures and Functions
PCT/US14/55430	PCT	9/12/2014	NA	Method for Atomic Layer Deposition
PCT/US14/56342	PCT	9/18/2014	United States	Torroidal Mesoporous Silica Nanoparticles (TMSNPs) and Related Protocells
14/555,453	Utility	11/26/2014	United States	Innovative Nanopore Sequencing Technology including a Self-Assembled Porous Membrane
61/977,238	Provisional	4/9/2014	United States	Safer-by-Design Doped Pyrogenic Silica Nanoparticles
62/130,392	Provisional	3/9/2015	United States	CD47 Containing Porous Nanoparticle-Supported Lipid Bilayers (Procels)
62/131,400	Provisional	3/11/2015	United States	Generation of Mesoporous Materials Using Multiphase Surfactant Systems
14/678,533	Divisional	4/3/2015	United States	Superhydrophobic Aerogel That Does Not Require Per-Fluoro Compounds or Contain any Fluorine
14/682,543	Utility	4/9/2015	United States	Safer-by-Design Doped Pyrogenic Silica Nanoparticles
62/168,991	Provisional	6/1/2015	United States	Nanobiocomposite Compositions and Methods
14/795,366	Cont-in_part	7/9/2015	United States	Shape-Preserving Transformations of Organic

				Matter and Compositions Thereof
62/214,436	Provisional	9/4/2015	United States	Design and Application of Protocell Platform for CD4+ and CD8+ T Cell Vaccine
62/214,513	Provisional	9/4/2015	United States	Monosized Mesoporous Silica Nanoparticles and Supported Lipid Bilayer Nanoparticle for Biomedical Applications
14/781,765	National	10/1/2015	United States	Mesoporous Alum Nanoparticles as a Universal Platform for Antigen Adsorption, Presentation, and Delivery
US 8,992,984	Utility	3/31/2015	United States	Protocells and Their Use for Targeted Delivery of Multicomponent Cargos to Cancer Cells
US 9,040,435	National	5/26/2015	United States	Superhydrophobic Aerogel That Does Not Require Per-Fluoro Compounds or Contain any Fluorine
US 9,242,210 B1	Utility	1/26/2016	United States	Enzymatically Active High-Flux Selectively Gas-Permeable Membranes
9,273,305	Utility	3/1/2016	United States	Cell-Based Composite Materials with Programmed Structures and Functions
9,249,333	Divisional	2/2/2016	United States	Durable Polymer Aerogel Based Superhydrophobic Coatings: A Composite Material
9,480,653 14	Divisional	11/1/2016	United States	Protocells and Their Use for Targeted Delivery of

				Multicomponent Cargos to Cancer Cells
62/323,445	Provisional	4/15/2016	United States	Engineering Bacterial Membranes with Rare Earth Phosphate Nanostructures
PCT/US2016/35289	PCT	6/1/2016	NA	Nanobiocomposite Compositions and Methods
PCT/US2016/50260	PCT	9/2/2016	United States	Mesoporous Silica Nanoparticles and Supported Lipid Bilayer Nanoparticles for Biomedical Applications (TMSNPs) and Related Protocells

## 4.7 Interactions/Transitions

**4.7.1 Biomolecular and Cellular Integration - Luna Innovations**, TPOC Blaine Butler – Our silicate immobilization and orthogonal platform technologies have been transitioned to Blaine Butler at Luna Innovations. There, Blaine has adapted our process to the immobilization of bacteria, yeast, and several fragile mammalian and fish cell lines. Specifics are as follows:

- Countering the Biothreat: Stabilizing CANARY Cells within 3D Nanomaterials for Real-Time & Robust Chem/Bio Agent Detection
  - Defense Threat Reduction Agency Invited White Paper with Jason Harper (SNL), Fran Nargi (MIT Lincoln Labs), and Blaine Butler (Luna Innovations)
  - TPOC Ilya Elashvile – still under consideration.

**4.7.2 Angstrom Thin Film Technologies LLC** - Plasma-Assisted Atomic Layer Deposition (PA-ALD) and Molecular Layer Deposition (MLD) - Partially supported by the AFOSR, was the development of PA-ALD to modify mesoporous thin films prepared by our evaporation-induced self-assembly process. The development of PA-ALD and more MLD was the basis of a startup company called Angstrom Thin Film Technologies LLC, which is building and selling ALD tools and also applying ALD-based technologies to solve problems associated with water purification and gas separation membrane

applications. Recently, we transferred the technology of peptide ALD to Angstrom Thin Film Technologies LLC, who are using this technological for low cost CO<sub>2</sub> separation membranes and water purification.

#### **4.7.2.1 Approach:**

- Ultra-thin (5-10 nm) watery membrane stabilized with nano pores
- Concentrated CO<sub>2</sub> enzyme absorbed on nanopores
- Enzyme-catalyzed rapid and selective CO<sub>2</sub> transport

#### **4.7.2.2 Accomplishments:**

- nm-thick enzyme-catalyzed membrane fabricated based on EISA mesoporous silica and plasma / ALD
- 500-2600GPU permeance and >500 CO<sub>2</sub>/N<sub>2</sub> selectivity achieved, satisfying DOE requirements
- Theoretical modeling further demonstrated nanopore enhanced enzymatic activity by multiple folds, demonstrating that membrane performance can be further improved

#### **4.7.2.3 Impact – 2015 R&D 100 Awards**

- Provides a potential solution for cost-effective CO<sub>2</sub> capture.
- Same idea may be used for oxygen membrane
- US patent was awarded – January 26, 2016
- Earned Gold Award in Green Technology: R&D 100 Green Technology Special Recognition Award.

## **5.0 References cited in the report**

1. Johnson, P. E.; Muttill, P.; MacKenzie, D.; Carnes, E. C.; Pelowitz, J.; Mara, N. A.; Mook, W. M.; Jett, S. D.; Dunphy, D. R.; Timmins, G. S.; Brinker, C. J., Spray-Dried Multiscale Nano-biocomposites Containing Living Cells. *ACS Nano* **2015**, *9* (7), 6961-77.
2. Kaehr, B.; Townson, J. L.; Kalinich, R. M.; Awad, Y. H.; Swartzentruber, B. S.; Dunphy, D. R.; Brinker, C. J., Cellular complexity captured in durable silica biocomposites. *Proc Natl Acad Sci U S A* **2012**, *109* (43), 17336-41.
3. Ashley, C. E.; Carnes, E. C.; Phillips, G. K.; Padilla, D.; Durfee, P. N.; Brown, P. A.; Hanna, T. N.; Liu, J.; Phillips, B.; Carter, M. B.; Carroll, N. J.; Jiang, X.; Dunphy, D. R.; Willman, C. L.; Petsev, D. N.; Evans, D. G.; Parikh, A. N.; Chackerian, B.; Wharton, W.; Peabody, D. S.; Brinker, C. J., The targeted delivery of multicomponent cargos to cancer cells by nanoporous particle-supported lipid bilayers. *Nat Mater* **2011**, *10* (5), 389-97.

4. Ashley, C. E.; Carnes, E. C.; Epler, K. E.; Padilla, D. P.; Phillips, G. K.; Castillo, R. E.; Wilkinson, D. C.; Wilkinson, B. S.; Burgard, C. A.; Kalinich, R. M.; Townson, J. L.; Chackerian, B.; Willman, C. L.; Peabody, D. S.; Wharton, W.; Brinker, C. J., Delivery of small interfering RNA by peptide-targeted mesoporous silica nanoparticle-supported lipid bilayers. *ACS Nano* **2012b**, *6* (3), 2174-88.
5. Butler, K. S.; Durfee, P. N.; Theron, C.; Ashley, C. E.; Carnes, E. C.; Brinker, C. J., Protocells: Modular Mesoporous Silica Nanoparticle-Supported Lipid Bilayers for Drug Delivery. *Small* **2016**, *12* (16), 2173-85.
6. Townson, J. L.; Lin, Y. S.; Chou, S. S.; Awad, Y. H.; Coker, E. N.; Brinker, C. J.; Kaehr, B., Synthetic fossilization of soft biological tissues and their shape-preserving transformation into silica or electron-conductive replicas. *Nat Commun* **2014**, *5*, 5665.
7. Harper, J. C.; Khripin, C. Y.; Khirpin, C. Y.; Carnes, E. C.; Ashley, C. E.; Lopez, D. M.; Savage, T.; Jones, H. D.; Davis, R. W.; Nunez, D. E.; Brinker, L. M.; Kaehr, B.; Brozik, S. M.; Brinker, C. J., Cell-directed integration into three-dimensional lipid-silica nanostructured matrices. *ACS Nano* **2010**, *4* (10), 5539-50.

# AFOSR Deliverables Submission Survey

Response ID:7576 Data

1.

**Report Type**

Final Report

**Primary Contact Email**

Contact email if there is a problem with the report.

cjbrink@sandia.gov

**Primary Contact Phone Number**

Contact phone number if there is a problem with the report

505-272-7627

**Organization / Institution name**

University of New Mexico

**Grant/Contract Title**

The full title of the funded effort.

Biocompatible and Biomimetic Self-Assembly of Functional Nanostructures

**Grant/Contract Number**

AFOSR assigned control number. It must begin with "FA9550" or "F49620" or "FA2386".

FA9550-14-1-0066

**Principal Investigator Name**

The full name of the principal investigator on the grant or contract.

C. Jeffrey Brinker

**Program Officer**

The AFOSR Program Officer currently assigned to the award

Dr. William P. Roach

**Reporting Period Start Date**

02/01/2014

**Reporting Period End Date**

01/31/2017

**Abstract**

Our bio-compatible and biomimetic research has been focused on the use of living cells, biomolecular-interfaces and bio-mimetic processes to direct the formation of new classes of complex, symbiotic, hierarchical materials with life-like structure and functionality. This aim is predicated on two principal goals: 1) use of living/fixed cells to direct the formation of new classes of complex, hierarchical materials with life-like (or new) structures and functionality, evidenced by the preservation of cell and organism structure in silica with sub 10-nm fidelity through a reaction with silicic acid, and transformation of these replicates to carbon or carbon/silica hybrids, enabling multiscale imaging without loss of resolution and 2) use of self-assembly to create engineered nano-to-microscale environments to direct new cellular behavior and confer enhanced biomolecular stability. These goals are premised on three key nano-to-microscale strategies pioneered by our team: silica cell replication (SCR), protocell platform for synthetic biology, cellular and biomolecular immobilization or stabilization using evaporation-induced self-assembly (EISA) and atomic layer deposition (ALD) and creation of biotic/abiotic interfaces through the interaction of rare earth oxides with bacterial membranes and metal organic framework (MOF) functionalization of mammalian cells. SCR provides a versatile means to form an exact silica replica of cells (as well as tissues

DISTRIBUTION A: Distribution approved for public release.

and complete organisms) with preservation and protection of shape and many aspects of extra- and intracellular biofunctionality upon complete drying. Preserved biofunctional properties include integrity of cell surface antigens, receptor-ligand binding and enzymatic activities. Development of the protocell platform for synthetic biology provides a means for characterizing the dynamics and phase behavior of supported lipid bilayers on silica cell replicas or porous silica particles to create synthetic membranes that capture key aspects of natural cell systems. Using the protocell platform, we rebuilt red blood cells (RRBCs) like material from natural red blood cells and demonstrated ability of our RRBC to maintain the curvature of the natural red blood cell (RBC) and circulate easily in the blood vessels of the Ex-Ovo chicken embryo (CAM). Through 3D cellular and biomolecular immobilization or stabilization, we completed the first genome wide, longitudinal evaluation of confinement induced behavioral changes in *S. cerevisiae* cells integrated into 3D silica matrices and established genomic changes consistent with persister-like cellular state. We also confirmed entrapment of carbonic anhydrase in a hydrophilic membrane fabricated through a combination of EISA and ALD, creating a CO<sub>2</sub> separation membrane with exceptional activity. For modification of bacteria with rare earths, we established universal modification of bacterial organisms by rare earths, giving rise to a new living biotic/abiotic phenotype with a unique combination of properties including insolubility, low toxicity, and optical activity following 'doping' with optically active rare earth ions of Eu. We determined qualitatively and quantitatively, the influence of rare earth modification on bacterial growth, induced metabolic changes, oxidative stress, enzymatic activity and bacterial behaviors including swarming, swimming motilities, and biofilm formation. We also confirmed lack of recognition of rare earth phosphate modified bacteria by mouse macrophage Raw264.7 cells. On MOF functionalization of mammalian cells, we established that MOF induces spore-like hibernation state by providing an exoskeletal protective coating which can prevent cell attachment and replication but allow transport of nutrients to ensure cell viability. On the basis of these findings, we believe that we have discovered important functional materials and revealed new functionalities and behaviors that can be important to sensing, energy harvesting, and adaptation to extreme environments of potential interest to the US Air Force.

#### **Distribution Statement**

This is block 12 on the SF298 form.

Distribution A - Approved for Public Release

#### **Explanation for Distribution Statement**

If this is not approved for public release, please provide a short explanation. E.g., contains proprietary information.

#### **SF298 Form**

Please attach your SF298 form. A blank SF298 can be found [here](#). Please do not password protect or secure the PDF. The maximum file size for an SF298 is 50MB.

[SF0298++AFOSR+Report+FA9550-14-1-0066+Brinker+2-1-2017.pdf](#)

**Upload the Report Document. File must be a PDF. Please do not password protect or secure the PDF. The maximum file size for the Report Document is 50MB.**

[AFOSR+Report+FA9550-14-1-0066+Brinker+2-1-2017.pdf](#)

**Upload a Report Document, if any. The maximum file size for the Report Document is 50MB.**

#### **Archival Publications (published) during reporting period:**

Included in the uploaded final report

#### **New discoveries, inventions, or patent disclosures:**

**Do you have any discoveries, inventions, or patent disclosures to report for this period?**

Yes

#### **Please describe and include any notable dates**

All patents generated from this work are included in the uploaded final report

**Do you plan to pursue a claim for personal or organizational intellectual property?**

Yes

**Changes in research objectives (if any):**

**Change in AFOSR Program Officer, if any:**

**Extensions granted or milestones slipped, if any:**

**AFOSR LRIR Number**

**LRIR Title**

**Reporting Period**

**Laboratory Task Manager**

**Program Officer**

**Research Objectives**

**Technical Summary**

**Funding Summary by Cost Category (by FY, \$K)**

	Starting FY	FY+1	FY+2
Salary			
Equipment/Facilities			
Supplies			
Total			

**Report Document**

**Report Document - Text Analysis**

**Report Document - Text Analysis**

**Appendix Documents**

**2. Thank You**

**E-mail user**

Feb 01, 2017 19:54:39 Success: Email Sent to: cjbrink@sandia.gov